

Final Report on
**Improving Prediction of Severe Winds, Convection and Heavy Precipitation
in the Southeastern United States**

to the

National Oceanic and Atmospheric Administration
Collaborative Science, Technology & Applied Research Program (CSTAR)
Award Number **NA10NWS4680007**

Department of Marine, Earth, & Atmospheric Sciences
North Carolina State University
Raleigh, North Carolina

July 2014

Contact: Gary M. Lackmann
Department of Marine, Earth, & Atmospheric Sciences
Box 8208
North Carolina State University
Raleigh, North Carolina 27695-8208
Phone: (919) 515-1439
Fax: (919) 515-7802
gary@ncsu.edu

List of Participants and Collaborators:

Principal Investigators - North Carolina State University:

Dr. Gary Lackmann
Dr. Matthew Parker
Dr. Anantha Aiyyer

Student Researchers:

Mr. Jason Davis – Graduated (MS) 2013
Mr. Jordan Dale – Graduated (MS) 2013
Mr. Keith Sherburn – Graduated (MS) 2013
Ms. Briana Gordon – Graduated (MS) 2011
Mr. Bryce Tyner – PhD Candidate

Collaborators within the National Weather Service:

Raleigh, North Carolina
Wilmington, North Carolina
Morehead City, North Carolina
Blacksburg, Virginia
Sterling, Virginia
Wakefield, Virginia
Greer, South Carolina
Charleston, South Carolina
Columbia, South Carolina
Peachtree City, Georgia
Huntsville, Alabama
NCEP Hydrometeorological Prediction Center (now Weather Prediction Center)
NCEP Storm Prediction Center
NCEP Tropical Prediction Center

Other Collaborative Partners:

Dr. Brian Etherton (RENCI, PI, year 1)

A. Project Overview

1.) Collaborative strategy time line

The success of collaborative research towards operational improvements requires meaningful engagement of both academic and operational personnel. Building on infrastructure and experience from previous CSTAR projects, we adopted an ambitious and creative model for an actively collaborative research process which emphasizes O2R and R2O interactions. We sought to avoid a one-way R2O model in favor of truly collaborative research between NCSU students and faculty and NWS personnel. Past experiences have demonstrated that this type of collaboration benefits from the identification and participation of *collaborative investigators* (CIs) on the NWS side. We implemented the following mechanisms as a foundation for our active collaboration approach:

- NWS CIs were identified at the outset of the project, and they played an active and integral role in research collaborations throughout the duration of the project;
- We developed and utilized a blog, entitled Collaboration for Improved Meteorology in the Mid-Atlantic and Southeast (CIMMSE), which was created by CSTAR students Bryce Tyner and Briana Gordon in collaboration with Raleigh SOO Jonathan Blaes. The blog functions to facilitate discussion of ongoing events and sharing of research results between PIs, students, and collaborators: <http://cimmse.wordpress.com>. As of July 2014, the blog hosted 297 posts in 17 categories with over 37,000 views; Sub-groups were organized for each research focus area, and regular meetings and teleconferences were held, involving NCSU PIs and students, and NWS CIs. Results and summaries from these calls and meetings are posted on the CIMMSE page;
- Regular regional CSTAR meetings were to be held, including an organizing workshop which was held at the beginning of the project (October 2010) to establish research directions. Due to travel restrictions which were imposed after the project start date, the year 2 and 3 meetings were held as teleconferences and virtual workshops.

Another crucial element to our collaborative structure was the involvement of three NCEP centers, which helped to increase the visibility and application of research findings on a national level. The Storm Prediction Center, Weather Prediction Center, and National Hurricane Center were all involved in the three research areas, discussed below. The Warning Decision Training Branch (WDTB) played an important role in dissemination of research results for the convective storms portion of the project. Overall, it is our sense that the collaborative model established as a part of this project was successful, and we plan to continue a similar model in future collaborations.

The proposed research included three main foci: (i) severe high-shear, low-CAPE (HSLC) convection, (ii) inland wind prediction during landfalling tropical cyclones (TCs), and (iii) inland precipitation prediction accompanying landfalling TCs. Specific research results relating to these three areas will be presented in detail in section B of the proposal.

The proposed work was completed during a 4-year period that included a 1-year no-cost extension, which was motivated by the need for additional time to disseminate research results.

Each of the research projects has now been completed, with four graduate students earning their degrees, and one continuing a PhD with support from this award during a 2-year period. The original project included four Principal Investigators, but one PI, Dr. Brian Etherton formerly of RENCI, departed in order to take a position with NOAA's Earth System Research Lab (ESRL) in Boulder, CO. After a discussion involving our NWS collaborators, the remaining PIs, students, and program manager Dr. Curtis Marshall, the funds formerly allocated to RENCI were used to recruit an additional graduate student, Mr. Jordan Dale, who worked in the same general project area where Dr. Etherton had been working, with an emphasis on tropical cyclone inland QPF.

The five graduate students supported by this award exceeded our original expectation of three. This was made possible by Dr. Etherton's departure, the use of teaching assistantship funds to supplement the research support from the CSTAR grant, and because two of the students, Jason Davis and Keith Sherburn, were selected for AMS Graduate Fellowship awards. See: <http://cimmse.wordpress.com/2012/01/27/two-nc-state-cstar-students-presented-with-ams-graduate-fellowships/>

2. Project highlights

- **Nationwide research dissemination:** Collaborations with National Centers proved beneficial during the course of this project. For example, in October 2013, graduate students Keith Sherburn and Jason Davis shared their research results via the first of two webinars. The first webinar was facilitated by the WDTB and was attended by a total of **62** different NWS offices including NWS headquarters and **57** different NWS WFOs. The total audience exceeded 190 NWS meteorologists from all four NWS CONUS regions. The audience contributed numerous questions and comments during the presentation. The presentation was recorded and archived, and is available on the WDTB web site. The second webinar was held in April 2014 with participants from more than 30 NWS offices with an audience of more than 100 NWS meteorologists. The presentation was added to the [NWS Eastern Region Headquarters Scientific Services YouTube channel](#).
- **TC wind collaboration with Tropical Hazards Team, GFE Developers:** At the 2011 NOAA Hurricane Conference, WFO RAH requested that the Tropical Hazards Team and GFE developers work with our CSTAR group to add additional science and improve collaboration in the creation of wind and wind gust grids associated with landfalling tropical cyclones by updating the TCMWindTool and creating a new TCWindGustTool. The topic was followed-up on at the 2013 NOAA Hurricane Conference and support was provided to the CSTAR group to develop an augmented version of the nationally supported TCMWindTool in GFE based on CSTAR research. The CSTAR group collaborated with developers and a set of new tools, along with documentation and reference materials, are available in several coastal NWS offices. The WindReductionFactor and GustFactor grids were operationally tested by three WFOs with Tropical Cyclone Andrea (2013), followed by a more rigorous test during Hurricane Arthur (July 2014).

- **Regional coordination meetings:** Activities began with a conference call on 4 August 2010, followed by a regional meeting held in Raleigh on 28–29 October 2010 (Fig. A1); this workshop featured CSTAR presentations of past and present research and discussions of current and upcoming collaborative research, and was attended by over 30 participants, with representatives from 9 collaborative NWS offices and 3 National Centers, in addition to NWS Eastern Region Headquarters. Project-wide coordination meetings were also held on 9 September 2011 and 16 November 2012; the 2011 meeting was held via teleconference, and the 2012 event was a virtual workshop. Additionally, quarterly planning and coordination meetings were held every three months and summaries of these meetings are available on the CIMMSE blog.



Figure A.1: CSTAR regional workshop attendees, 29 October 2010.

- **Online collaborative tools:** As of May 2014, the Collaboration for Improved Meteorology in the Mid-Atlantic and Southeast (CIMMSE) blog, <http://cimmse.wordpress.com>, had hosted 297 posts in 17 categories with over 37,000 views. A new NWS-NCSU Collaborative Research and Training Web Site has been developed: <http://sites.google.com/site/nwsncsucollab/home>.
- **Regular coordination and interaction:** Each of the three research-area groups conducted regular monthly conference calls led by the respective PI, students, and NWS collaborative investigator with participation from members of the sub-project team. Summaries of these calls and meetings are shared on the Collaboration for Improved Meteorology in the Mid-Atlantic and Southeast (CIMMSE) blog. Project participants are from NC State, 11 WFOs, and 3 national Centers with more 60 individual collaborators.

More than 25 of these collaborators regularly participated in conferencing calls or project activities. Quarterly planning and coordination meetings were generally held every three months and summaries of these meetings are also available on the CIMMSE blog.

- **Tool development and sharing:** Statistical analysis confirmed that a product of low-level lapse rates, mid-level lapse rates, and various wind and shear magnitudes provide a useful discriminator between HSLC significant severe and non-severe convection. This combined parameter has been dubbed the Severe Hazards in Environments with Reduced Buoyancy parameter, or SHERB. During the late evening of Halloween 2013, the Ohio Valley experienced a fairly widespread HSLC tornado outbreak. The SHERB, by then available to NWS forecasters, proved to be extremely valuable during this event. The NWS Wilmington OH (ILN) staff participated in the WDTB training a few days prior to the severe weather. After the event, the ILN SOO (Seth Binau) noted in a [blog post](#) that “the SHERB data was instrumental in raising awareness to the scope/magnitude of the event when traditional severe weather forecasts (SPC Outlooks, CAPE, etc.) were not as suggestive of a higher-end event.” This was a great example of the sharing local research results outside of our CSTAR cluster and across the NWS.
- **Seminars, webinars, posters, and presentations:** At least **20** seminars, webinars, conference presentations, and posters were delivered, based on CSTAR material (see section D). This included four MS thesis defenses, five webinars, five conference presentations at NWA and AMS meetings, and several seminars developed at regional workshops and NWS offices.
- **Research publications:** To date, three journal articles in Weather and Forecasting have been accepted for publication, with a fourth in preparation. Two of these articles, relating to HSLC environments, are in print.
- **Student professional development:** Of the four CSTAR students that completed their MS degrees during the course of this project, Jason Davis has recently gained employment with the NWS forecast office in Birmingham, AL. Former MS student Jordan Dale is now working for the US Department of Energy in Washington, DC, while 2011 graduate Briana Gordon is working for the private-sector firm Sonoma Technology, Inc. in California. After working in the private sector, former MS student Keith Sherburn is returning to NCSU to pursue a doctoral degree, beginning in the fall of 2014. Bryce Tyner is nearing the completion of his PhD degree. Were it not for the NWS hiring freeze during years 2 and 3 of the project, it is likely that additional CSTAR students would be working for the NWS.

The remainder of this report is organized as follows. First, in-depth research summaries are presented, with a subsection dedicated to each of the three primary research areas. A list of additional highlights is provided in section C, followed by a list of references. Personnel listed for the different sections only include those at NCSU, but at the end of the report, a complete listing of the NWS collaborators is provided.

B. Research Results

1.) High-shear, low CAPE convective storms (Davis, Sherburn, and Parker)

During the development of the original proposal, a problem that frequently emerged during discussions with NWS forecasters related to the prediction, nowcasting, and warning for severe storms in environments with large vertical wind shear but small instability (i.e. CAPE). Such high-shear/low-CAPE (hereafter, “HSLC”) severe storms may take the form of squall lines/bow echoes, which are common when lower tropospheric shear is large (e.g., Weisman 1993), and have been frequently observed during the cool season (Burke and Schultz 2004). Alternatively, HSLC severe storms may take the form of “miniature” (also known as “low topped”) supercells (e.g., Davies 1990; Kennedy et al. 1993). These HSLC outbreaks are often characterized by widespread severe wind reports, as well as some tornadoes. In particular, HSLC tornado days represent a very difficult forecasting challenge. Our operational partners had noted that such tornadoes are “difficult to identify on radar”, and they often occur during the cool season “when many people assume that severe convective storms are highly unlikely.” One office noted that this phenomenon “taxes the warning system to its utmost” and another stated that they need researchers “to help find better techniques for the forecasters” in dealing with HSLC storms. Clearly, the operational need provided ample motive for this work.

The HSLC problem is distinctly relevant in the southeastern US, where the mean tornado environment is characterized by CAPE values below 1000 J kg^{-1} (Fig. 1.1a). This is a small amount relative to that observed in the tornado environments of the Great Plains (i.e. the corridor from the Texas Panhandle through southeastern Nebraska in Figure 1.1a). The lower CAPE values are largely compensated by large vertical wind shear; tornado environments in the Southeast commonly exhibit 0-6 km bulk shear vector magnitudes (hereafter, “BSVM”) of $18\text{-}25 \text{ m s}^{-1}$, which is stronger than the mean deep-layer BSVM found over the Great Plains (Fig. 1.1a). McCaul and Weisman (1996) have shown that the dynamic contribution from vertical wind shear can overcome the apparent drawbacks of limited buoyancy, such that HSLC supercells can have updraft speeds that are nearly as large as those of high-CAPE storms. Unfortunately, the false alarm rates in these environments can be high, as HSLC conditions are present for many hours each year (Figure 1.1b).

The HSLC environment is also relevant to severe bow echoes/squall lines. Squall lines may produce severe winds via conventional mechanisms (as reviewed by Wakimoto 2001), but are also associated with embedded mesovortices (Trapp and Weisman 2003; Atkins et al. 2004; 2005; Wheatley et al. 2006), which enhance straight-line winds (Wakimoto et al. 2006; Atkins and St. Laurent 2009) and also can lead to tornadoes (Przybylinski 1995; Funk et al. 1999; Atkins et al. 2004; Trapp et al. 2005). Both Weisman and Trapp (2003) and Atkins and St. Laurent (2009) have shown that the occurrence of embedded mesovortices increases as the environmental shear increases (as in HSLC regimes).

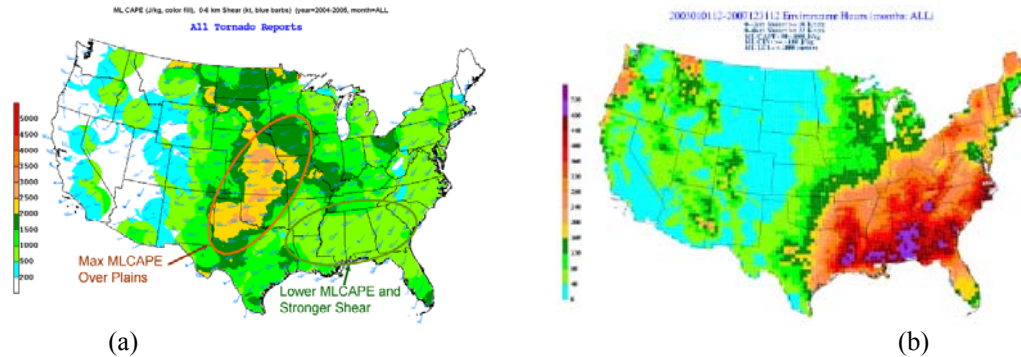


Figure 1.1: Depiction of the mean environments for storms over the continental US. a) Mean mixed layer CAPE (MLCAPE, shaded, $J\ kg^{-1}$) and 0-6 km BSV (barbs, kt) for all tornado reports in 2004 and 2005. b) Number of hours (totaled over the 5 year period 2003-2007) during which the local environment possessed low CAPE ($1000 > MLCAPE > 50\ J\ kg^{-1}$), but was otherwise favorable for tornadoes, including large low-level vertical shear (0-1 km BSV $> 10\ m\ s^{-1}$), large deep-layer wind shear (0-6 km BSV $> 18\ m\ s^{-1}$), small convective inhibition (MLCIN $> -100\ J\ kg^{-1}$), and low cloud base (MLLCL height $< 1000\ m$). Images provided by Steve Weiss of the SPC, derived from a database described by Schneider et al. (2006) and Schneider and Dean (2008).

One main research stream within the HSLC component involves the development of environmental indices to aid in understanding of the processes leading to severe HSLC events, and to equip operational forecasters with parameter-based tools to improve anticipation of severe events. Graduate student Keith Sherburn led this part of the HSLC research effort. Keith presented related work at the AMS SLS meeting (Nashville, TN) in November 2012, as well as at the NCSU-NWS Regional (virtual) Workshop held in November 2012 and the AMS 12th Annual Student Conference (Austin, TX) in January 2013. Keith submitted an article on this work to *Weather and Forecasting*, where it is currently in press (accepted in April 2014), and also successfully defended his MS thesis in May 2013.

The second focus area for this sub-topic is storm-scale radar analysis designed to improve both meteorological understanding and knowledge of the operational ability to distinguish severe and tornadic signatures from non-severe or non-tornadic HSLC convective events using radar. This work, led by graduate student Jason Davis, was also presented at the AMS Severe Local Storms conference and the NCSU-NWS Regional Workshop (both in November 2012). Jason defended his MS thesis in the summer of 2013, and after a brief stint in the private sector, has recently taken a position at the NWS forecast office in Birmingham, AL. Jason also submitted an article on this work to *Weather and Forecasting*, where it is currently in press (accepted in April 2014).

Following graduation, both Keith and Jason continued to work towards dissemination of their research. For example, in October 2013, they shared their research results via a WDTB webinar that was recorded and archived on the WDTB web site. Jason and Keith also delivered an additional webinar presentation entitled "Improving the Forecasting of Severe Weather in High Shear, Low CAPE Environments" on April 15, 2014. This presentation was attended by 29 different NWS offices.

Conference calls including Dr. Parker, the graduate students, and representatives from all of the collaborating regional WFOs continued to be held on a monthly basis throughout the project, led by Pat Moore and Justin Lane from WFO GSP. Almost all of the collaborating WFOs completed case studies of important HSLC events from their respective CWAs, and

these case studies have been formalized into reports that were subsequently shared with NCSU researchers and all other WFOs.

a.) Environmental Parameters Study

Towards the goal of developing indices to characterize and distinguish severe and non-severe HSLC environments, graduate student Keith Sherburn used gridded SPC mesoanalysis data (the “SFCOA”) to evaluate potential environmental discriminators. A journal article presenting this work was submitted to *Weather and Forecasting* in April, 2013 (Sherburn and Parker 2013), and is now accepted and *in press*. Repeated statistical analysis confirmed that of the environmental parameters tested in our development dataset, a product of low-level lapse rates, mid-level lapse rates, and various wind and shear magnitudes, provides the optimum discriminator between HSLC significant severe and non-severe convection. Keith created this composite parameter by taking the product of the three conditionally most skillful parameters in the development dataset, which were the effective shear magnitude (ESHR), the 700-500 mb lapse rate (LR75), and the 0-3 km lapse rate (LLLR). This parameter, referred to as the Severe Hazards in Environments with Reduced Buoyancy parameter – Effective shear version (SHERBE), is given by:

$$SHERBE = (ESHR/26 \text{ m s}^{-1}) * (LR75/5.8 \text{ K km}^{-1}) * (LLLR/5.2 \text{ K km}^{-1}). \quad (1.1)$$

Given that ESHR is dependent on CAPE, and considering that some of the significant events in our development dataset occurred with analyzed CAPE of 0 J kg^{-1} , the ESHR analysis may be suspect in some HSLC cases. Thus, we also evaluated the use of fixed-layer shear magnitudes in order to maximize skill. Through TSS calculations, it was determined that using the 0-3 km shear magnitude (S3MG) rather than ESHR improved skill in our development dataset. Thus, the Severe Hazards in Environments with Reduced Buoyancy parameter (SHERB) is defined:

$$SHERB = (S3MG/25 \text{ m s}^{-1}) * (LR75/5.8 \text{ K km}^{-1}) * (LLLR/5.2 \text{ K km}^{-1}). \quad (1.2)$$

These parameters were then tested using a verification dataset, which consisted of all significant severe reports across the entire U.S. from 2006 through 2011 and all nationwide nulls (as defined previously) between October 2006 and December 2011. Figure 1.2 shows a plot of TSS against different parameter threshold values for the SHERBE, SHERB, Significant Tornado Parameter (STP), Supercell Composite Parameter (SCP), Craven-Brooks Significant Severe Parameter, Vorticity Generation Parameter (VGP), and Energy Helicity Index (EHI).

Noteworthy features of Figure 1.2 are that first, within our CSTAR domain, the SHERB and SHERBE are more skillful than existing composite parameters at discriminating between all HSLC significant events and nulls. Secondly, though the existing composite parameters exhibit skill, their optimal skills occur at values lower than previously deemed operationally useful. For example, Thompson et al. (2004) noted that the optimal value for the STP was 1, where in our dataset, it is approximately 0.2. Even when comparing only HSLC significant tornadoes against nulls (not shown), the SHERB and SHERBE outperform other existing composite parameters designed specifically to identify environments capable of producing significant

tornadoes, and the optimal values for other parameters are low compared to previous knowledge.

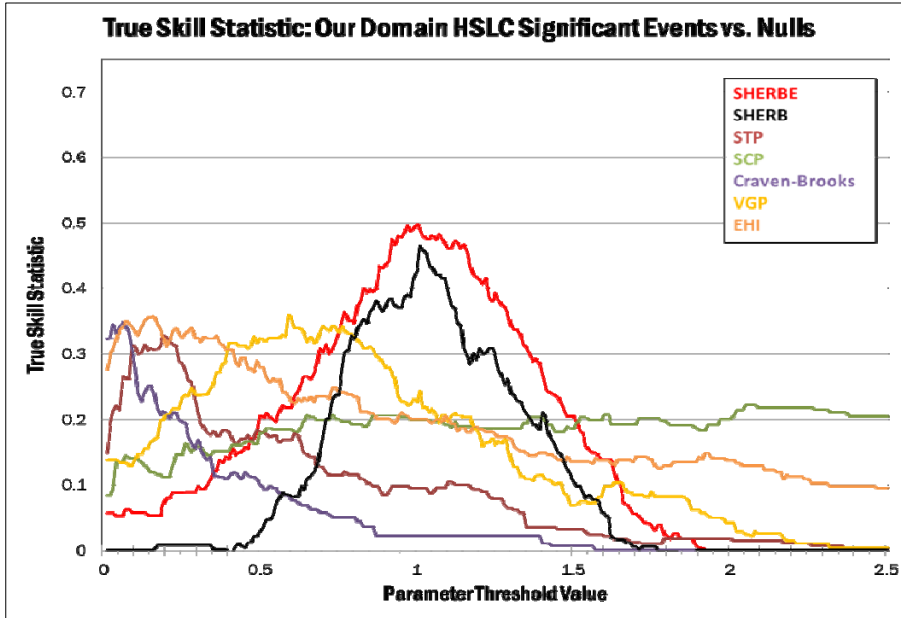


Figure 1.2. True skill statistic in discriminating HSLC significant reports from nulls as a function of parameter threshold value for the composite parameters listed in our CSTAR domain using the verification dataset. Note that the Craven-Brooks values are normalized by 50000, while the VGP values are normalized by 0.1.

As the research process evolved during the course of the project, HSLC environmental climatology research shifted from a focus on development (through use of specific cases identified by our regional WFO collaborators) to a focus on verification of new forecasting techniques (through use of all HSLC reports and null events nationwide). This included developing a nationwide climatology of HSLC significant severe events. Across the contiguous U.S., there are noteworthy annual and regional cycles in HSLC events, as well as regional differences in primary HSLC severe report types (Fig. 1.3). These transitions suggest that there are multiple HSLC regimes of significant severe weather. Further research has shown that HSLC events commonly take one of three forms: surface-based, low LCL convection (typical Southeast/Mid-Atlantic variety), elevated convection (low surface-based CAPE but large elevated instability), and high-based convection (especially common in the High Plains and Rockies in association with dry, well-mixed boundary layers). These findings were substantiated by the distributions of environmental parameters associated with the events (Fig. 1.4).

The most skillful wind or shear magnitude varies by the synoptic regime, region, and season. For example, the 6-km wind magnitude is the most skillful kinematic ingredient (when coupled with the lapse rates) at discriminating between cool season significant wind events and non-severe events. This is likely indicative of the importance of downward momentum transfer in addition to large system propagation speeds in strongly-forced cool season events. The ultimate goal of the study was to find a parameter that had optimal skill cutting across all regimes, regions, and seasons.

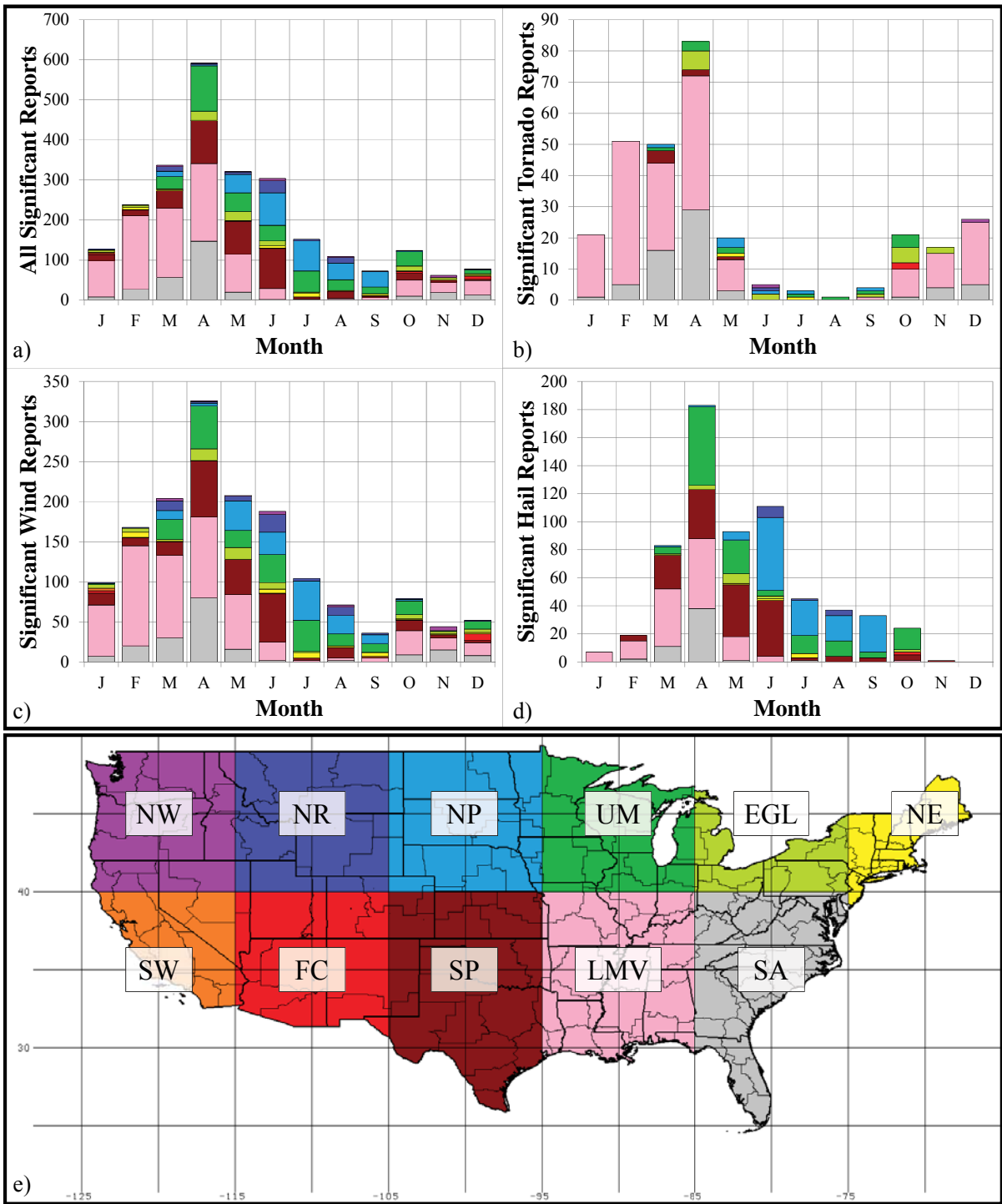


Figure 1.3. Annual cycles of a) all HSLC significant severe reports, b) HSLC significant tornado reports, c) HSLC significant wind reports, and d) HSLC significant hail reports by regions. e) Subjectively-defined regions as referred to in the text. Region labels: NW – Northwest; NR – Northern Rockies; NP – Northern Plains; UM – Upper Midwest; EGL – Eastern Great Lakes; NE – Northeast; SW – Southwest; FC – Four Corners; SP – Southern Plains; LMV – Lower Mississippi Valley; SA – South Atlantic. Colors in bar graphs correspond to region colors in e).

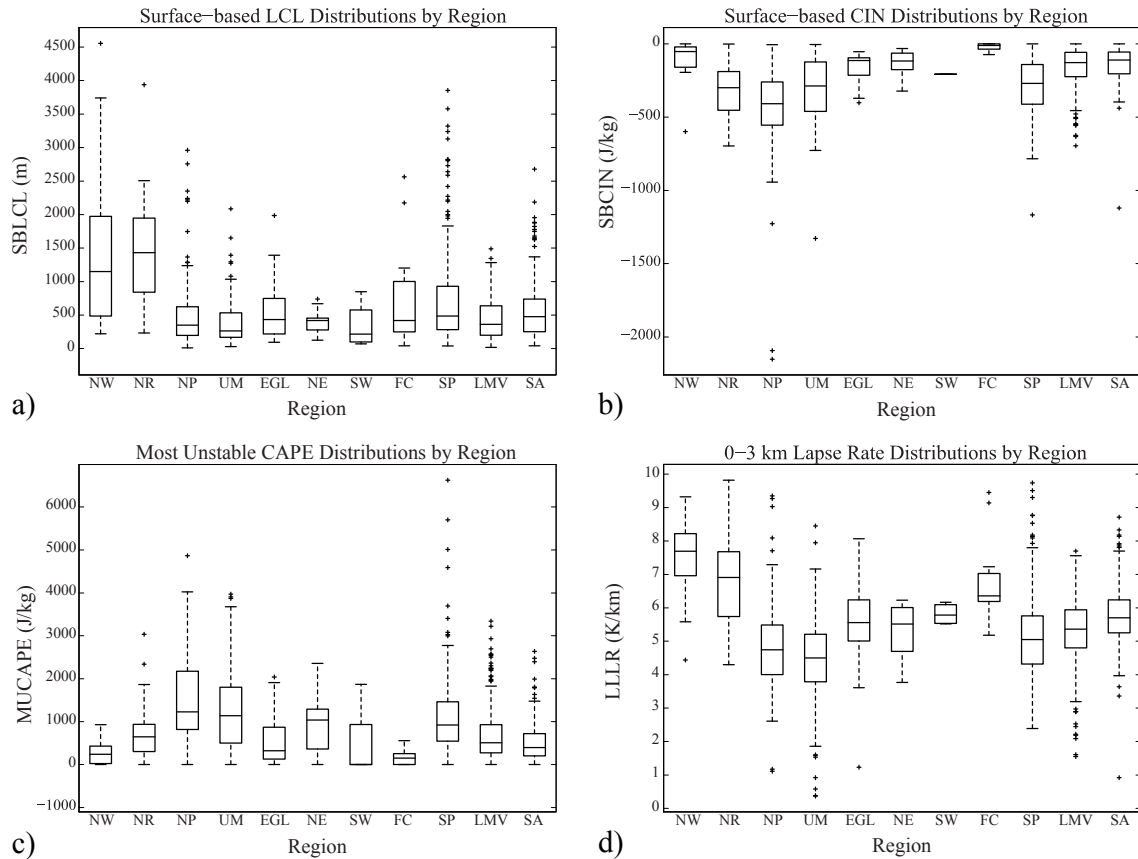


Figure 1.4. Box-and-whisker plots showing the distributions of a) SBLCL, b) SBCIN, c) MUCAPE, and d) LLLR for all HSLC significant wind reports by region. Regions are defined in Fig. 2.1. 25th and 75th percentiles are noted by the box, with the median noted by a horizontal line within the box. Whiskers extend to the 10th and 90th percentiles, and additional outliers are plotted as crosses.

The SHERB (a.k.a. SHERBS3) and SHERBE show particular skill in the Lower Mississippi Valley and South Atlantic regions, though there are multiple regions where one of these two parameters is the most skillful at discriminating between HSLC significant severe reports and nulls (Fig. 1.5). Distributions of the SHERBS3 and SHERBE for events and nulls are shown in Fig. 1.6. The parameters are most skillful at discriminating between significant tornadoes and nulls, and the SHERBE does particularly well at determining environments favorable for HSLC significant hail events. However, both parameters struggle with identifying significant wind environments, likely due to the myriad of environments capable of producing such events. An important finding is that the SHERB parameters generally outperform existing severe weather indices (Fig. 1.6), such as the Significant Tornado Parameter (STP), Supercell Composite Parameter (SCP), Craven-Brooks Significant Severe Parameter, Vorticity Generation Parameter (VGP), and Energy Helicity Index (EHI). As mentioned above for regional results, even when the previous severe weather indices are skillful in certain HSLC regimes, we find that their values are much lower than the conventional threshold for which they were designed to be used (often, the values would not even be contoured in the SPC mesoanalysis images, for examples).

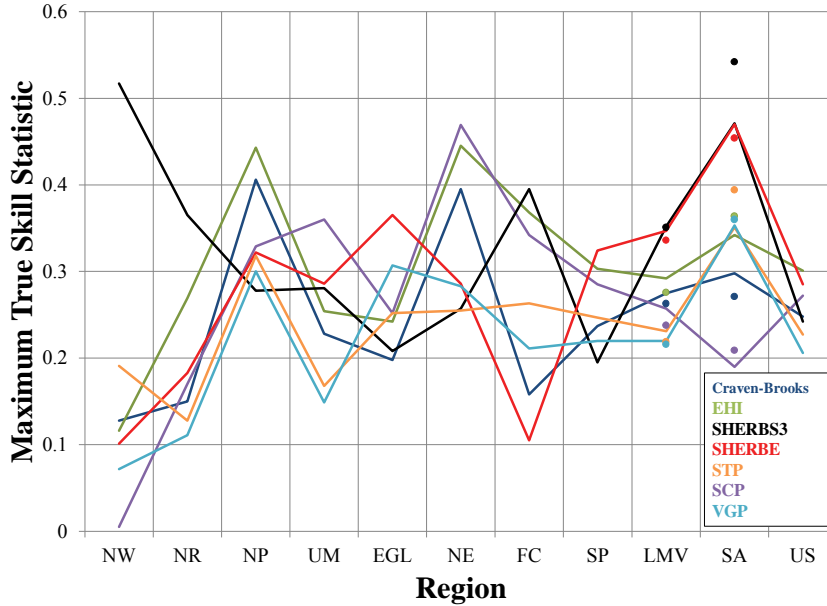


Figure 1.5. Maximum true skill statistic for given composite parameters at discriminating between HSLC significant severe reports and nulls across all regions and entire U.S. Dots indicate those statistics calculated without including reports and nulls from collaborating county warning areas in regions LMV and SA, ensuring a truly independent dataset. Region SW is excluded due to a very small sample size.

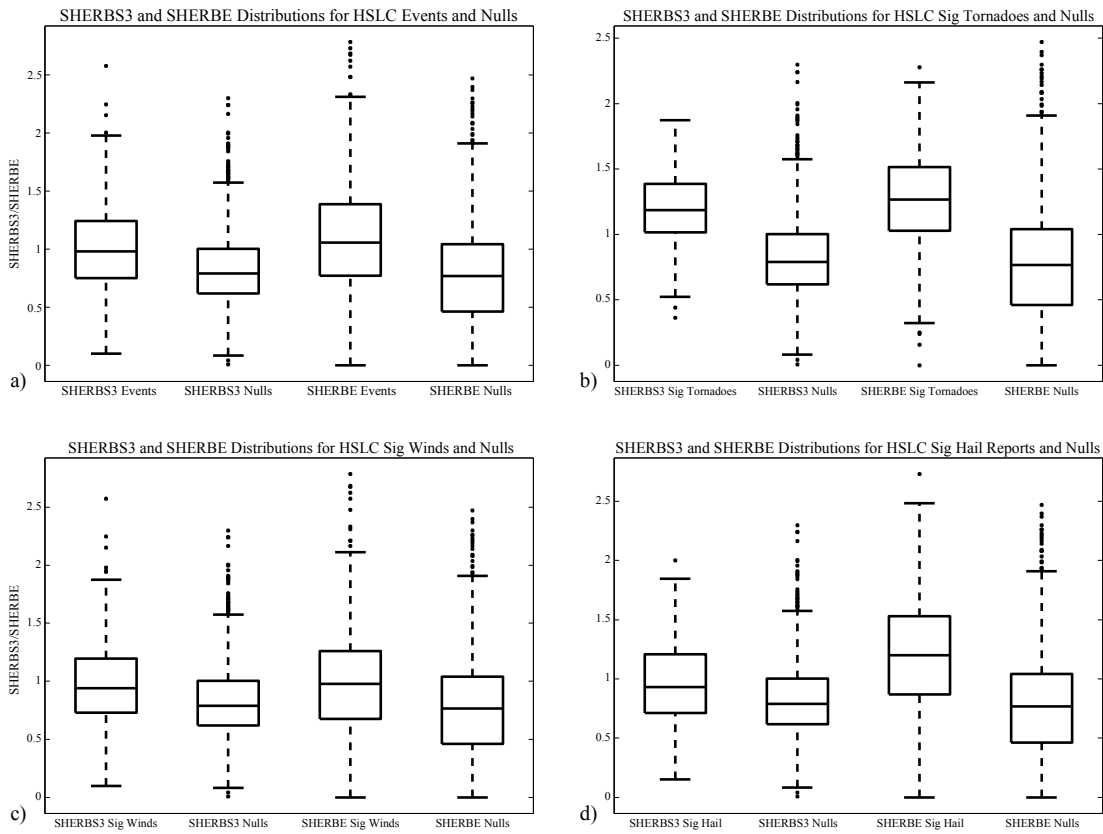


Figure 1.6. SHERBS3 and SHERBE distributions for a) all significant HSLC events and nulls, b) significant HSLC tornadoes and nulls, c) significant HSLC wind events and nulls, and d) significant HSLC hail events and nulls within the verification dataset. Plots are defined as in Fig. 1.4.

b.) Radar Signatures Study

Investigation of radar signatures differentiating severe and non-severe HSLC events was led by graduate student Jason Davis, who defended his thesis in July, 2013. The primary outcome of this work was the discovery of statistically significant differences in azimuthal shear between HSLC tornadic and non-tornadic vortices within 60 km of the radar, particularly in the lower elevation scans (near the surface). A journal article presenting this work was submitted to *Weather and Forecasting* in October, 2013 (Davis and Parker 2013), and is now accepted and *in press*.

Preliminary analysis of convective modes for the radar climatology portion of the HSLC project involved scrutiny of over 100 days between 2006 and 2011 that were identified by area WFOs as possible HSLC events. Tornadoes that occurred in an environment with surface-based CAPE (SBCAPE) less than 500 J/kg were included in the analysis. SBCAPE was determined from gridded hourly SPC mesoanalysis data. A total of 302 tornadoes on 59 of the days in the HSLC case list met this criterion. As some days may have contained HSLC environments in some areas of the domain but higher CAPE environments in other locations, this helps to ensure that only true HSLC tornadoes were included.

Convective mode information was obtained for these tornadoes from the Storm Prediction Center's (SPC's) convective mode database. Due to initial spatiotemporal filtering applied to the database, convective mode information was available for only 226 of the 302 HSLC tornadoes. Convective mode was manually assigned retrospectively to these tornadoes by SPC forecasters. Storms were classified as either supercells or non-supercells based on the presence of an area of rotation that met mesocyclone criteria, as well as other radar reflectivity signatures present in volumetric radar data. Sub-classifications for supercells included discrete supercell, supercell in cluster, and supercell in line. Non-supercells that met quasi-linear convective system (QLCS) criteria were classified accordingly (tornadoes classified as QLCS tornadoes therefore are not associated with mesocyclones). Tornadoes in a convective line that were associated with a mesocyclone were classified with the "supercell in line" designation. More information on this classification scheme can be found in Smith et al. (2012).

Figure 1.7 shows the distribution of convective modes for the 226 HSLC tornadoes in our dataset. The majority of HSLC tornadoes were associated with supercells, but there is a substantial fraction of HSLC QLCS tornadoes. Discrete supercells make up a relatively small percentage of HSLC supercell tornadoes, with supercells in clusters and supercells embedded in convective lines making up the majority of HSLC supercell tornadoes.

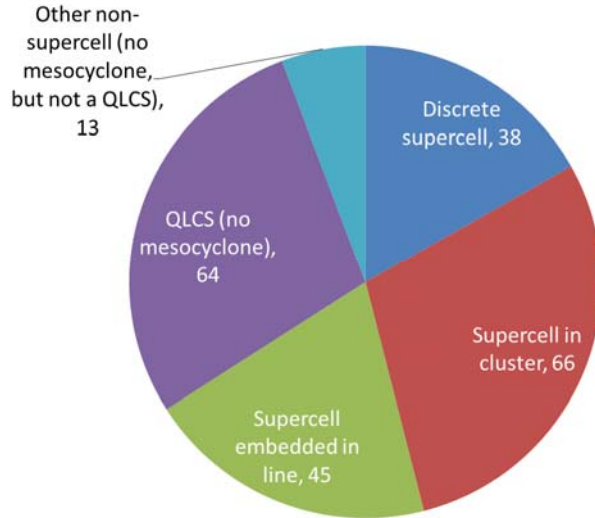


Fig. 1.7: Distribution of convective modes associated with a dataset of 226 tornadoes occurring in the Southeast under SBCAPE of 500 J/kg or less.

A tracking algorithm was developed and tested in order to study temporal and vertical trends in the strength of HSLC mesocyclones/mesovortices (hereafter more generically referred to as vortices). Azimuthal shear was used to diagnose the strength of these vortices, using radial velocity data from the nearest WSR-88D radar to the vortex. The main emphasis in this portion of the project was to seek discriminating factors in azimuthal shear between tornadic and non-tornadic vortices, by studying a relatively large number of cases. This part of the project also sought to identify the potential lead time for HSLC tornadoes, and determine what radar velocity information is most important for forecasters to focus upon. A total of 83 unique tornadic vortices and 84 non-tornadic vortices (determined using false alarm warnings) have been successfully tracked (Fig. 1.8), using HSLC cases that occurred after the WSR-88D radars were upgraded to produce “super-resolution” velocity products in mid-2008.

The vortex tracking algorithm was finalized and the vortex positions were manually quality-controlled. Following analysis of the final, quality assured data, some themes arose that are important for detection and warnings of HSLC vortices. These discriminating factors between tornadic and non-tornadic vortices include variables such as azimuthal shear, delta-V (the difference between maximum inbound and outbound velocities), and vortex diameter. The reflectivity features associated with each vortex have also been subjectively reviewed and classified for each tracked vortex. We therefore have a rich database of 95 tornadic vortices and 135 non-tornadic vortices for assessing the probability of detection and false alarm rate, as well as typical lead time, associated with various rotational thresholds and reflectivity signatures.

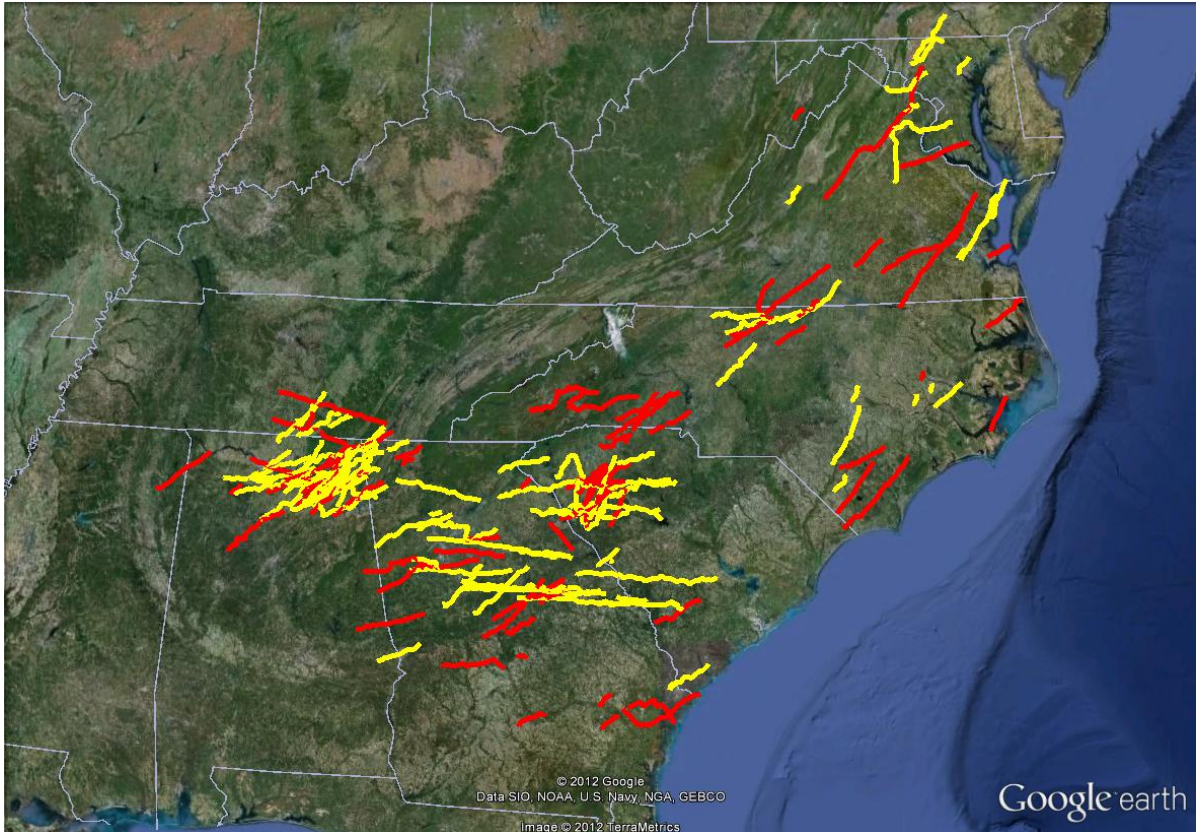


Figure 1.8 Tracks of the 83 tornadic vortices (yellow) and 84 non-tornadic vortices (red) that were tracked by the tracking algorithm.

A summary of the median vortex lifetimes and lead times using different azimuthal shear thresholds is presented in Table 1.1. In general, tornadic vortices are longer-lived than non-tornadic vortices (although, of course, an operational forecaster won't know how long a vortex will live in real time). Reassuringly, though, the somewhat long lifetimes of the tracked vortices imply the possibility of non-negligible warning lead time. This is especially true for supercell vortices, which tend to be much longer-lived than their QLCS counterparts, and which also tend to be associated with much greater potential lead times (Table 1.1). Indeed, even at very low thresholds, the median lead time for tornadoes from detected QLCS vortices is 5 minutes. Even so, QLCS mesovortices normally lived for at least 10-20 minutes (Table 1.1), implying that such phenomena are at least fundamentally detectable and trackable in real time. Lifetimes and lead times decrease for higher azimuthal shear thresholds as expected, but higher thresholds also remove more of the non-tornadic vortices. It appears that an azimuthal shear threshold of 0.01 s^{-1} provides a nearly optimal combination of 5-15 minutes of lead time (depending upon storm type) combined with exclusion of most non-tornadic vortices.

Owing to the fact that lifetimes and lead times are only known after the event, we have also emphasized use of time series of fundamental, derived velocity variables (such as azimuthal shear). The best separation between tornadic and non-tornadic vortices is found within 60 km of the radar site, where higher radar resolution and lower radar beam height combine to best sample the low-level vortices. In the lowest two scan elevations (0.5 and 0.9 degrees), this separation is rather dramatic during the 10 minute prior to tornado touchdown (Fig. 1.9).

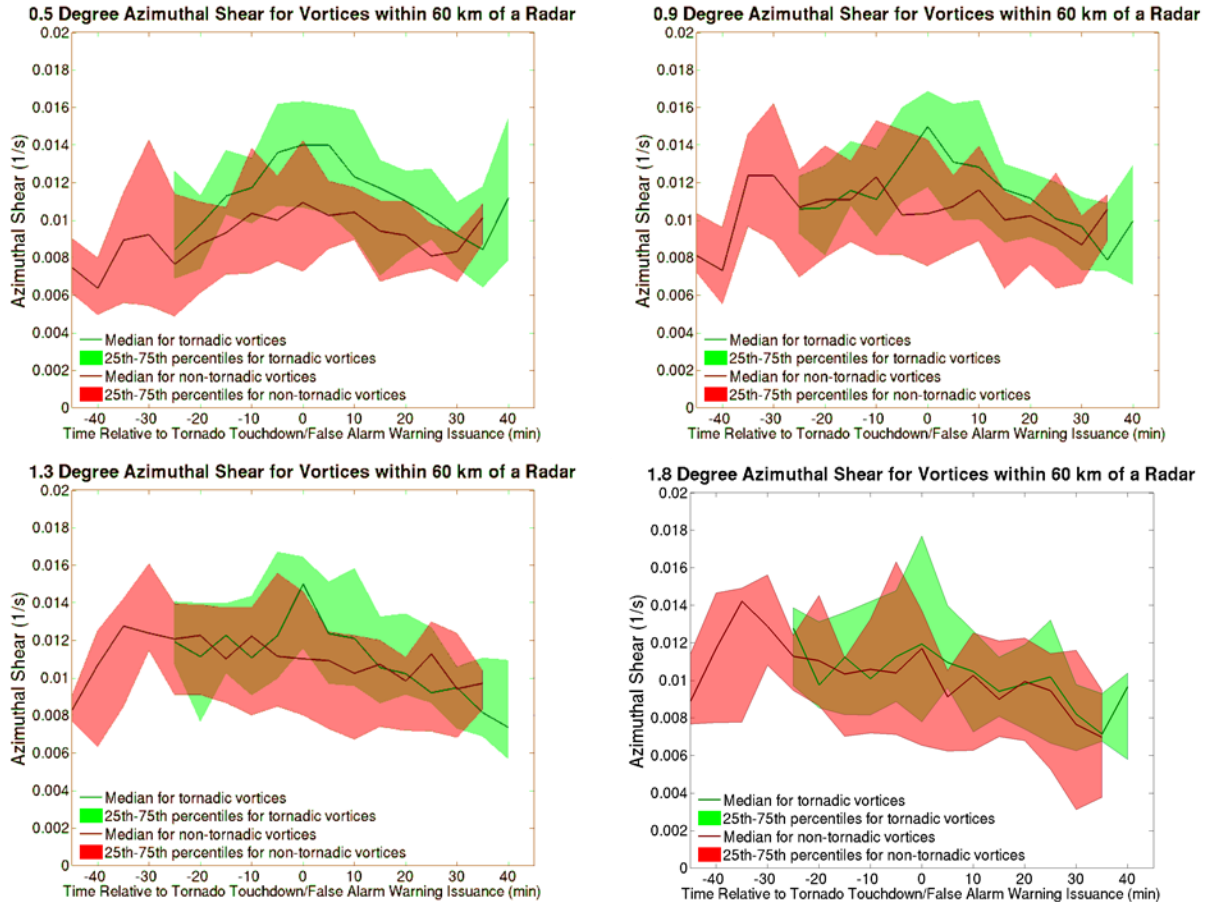


Figure 1.9: Distribution of azimuthal shear vs. time for all tornadic (green, $n=32$) vs. non-tornadic (red, $n=29$) vortices tracked in this study. The distributions are shown for the lowest four elevation scans (0.5, 0.9, 1.3, and 1.8 degrees). For tornadoes, $t=0$ min is equivalent to the reported starting time of the tornado. For non-tornadic vortices, $t=0$ min is equivalent to the starting time of the NWS-issued warning. The shaded zones correspond to the middle 50% of the distributions, with the medians indicated by solid lines. Only vortices from within 60 km of the radar are included here.

At both tornado time and 5 minutes prior to tornado time, these differences are statistically significant at the 95% confidence level (not shown). Strangely, although some separation is visible in the distribution for supercells (Fig. 1.10), none of these differences are statistically significant, even in the base scan, *at* tornado time. This may be indicative of the generally stronger nature of non-tornadic mesocyclones in supercells. However, given our perception that QLCS tornadoes are a much greater operational challenge, it is quite promising that there is excellent separation between the tornadic and non-tornadic QLCS vortices (Fig. 1.11), and these differences in the lowest 2 elevation scans are statistically significant at the 95% confidence level at both $t=0$ min (tornado time) and $t=-5$ min. Thus, it may be possible to use a shear threshold to skillfully issue warnings for QLCS tornadoes. Also promising is that the separation (both visually and as measured by statistical tests of significance) between EF1+ tornadoes and nulls is even better in the 0-60 km range (Fig. 1.12), implying that forecasters have a very good chance of detecting more substantial tornadoes by applying a threshold, without having to tolerate exceedingly large numbers of false alarms. In fact, the EF1+ tornadoes are also associated with better separation in the higher elevation scans as well (Fig. 1.12), and these differences aloft are statistically significant at the 95% confidence level at $t=0$ min (tornado time).

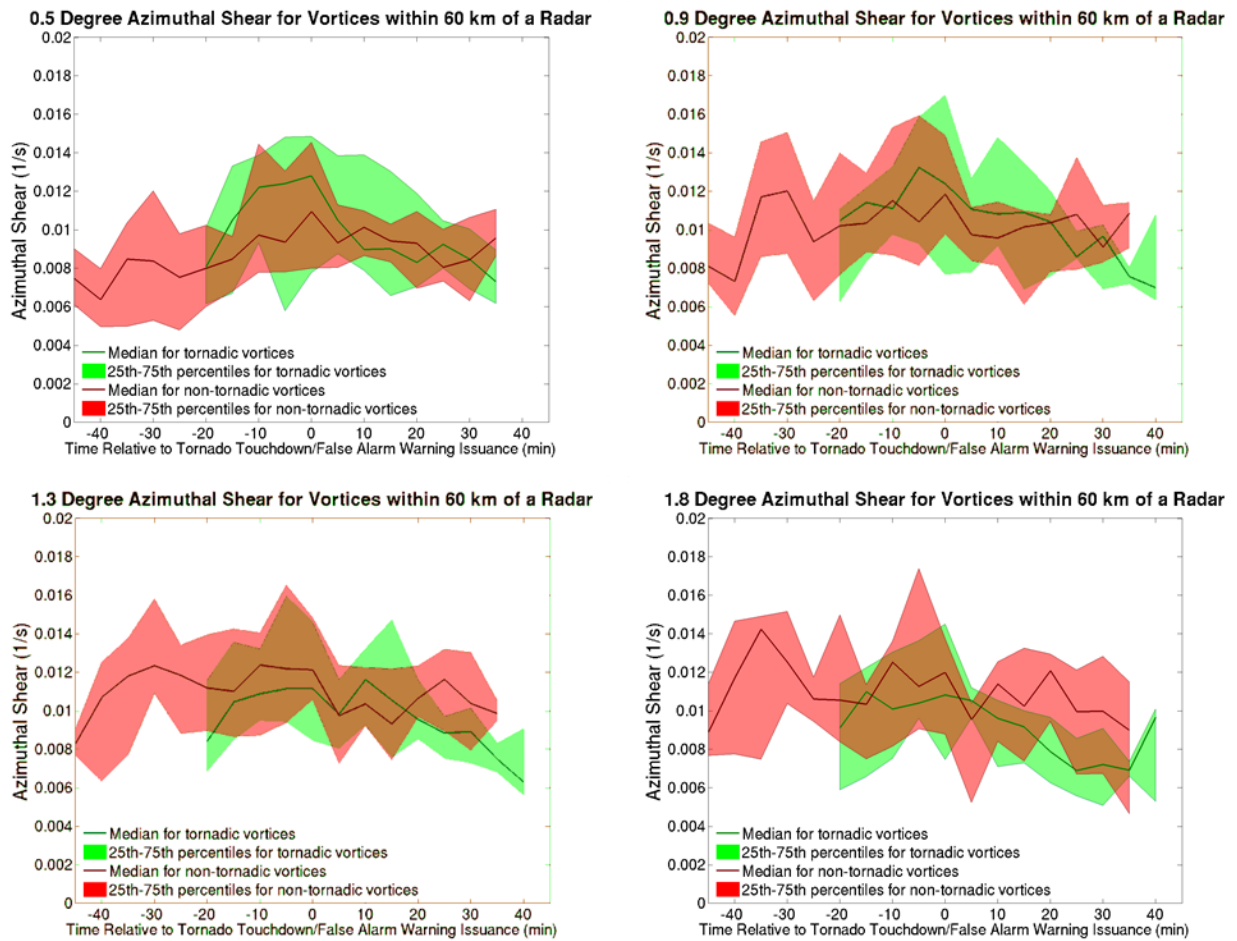


Figure 1.10: Same as Figure 1.9 except only for tracked supercells (including 9 tornadic and 12 non-tornadic vortices).

Unfortunately, at greater distances from the radar, the findings are not as promising. Although not shown, plots and statistical tests for the 60-100 km and 100+ km range bins reveal very few useful signals. Interestingly, there is some statistical significance *aloft* for supercells and also EF1+ tornadoes in the more distant range bins. The radar is likely not sampling the near-surface vortex very well at these distances, but it is possible that the tornadic vortices are associated with deeper storms (and/or deeper mesocyclones) which are better sampled by the more elevated radar beam at these distances. Notably, due to decreasing effective resolution of the radar, there is a noticeable decrease in the distribution of observed azimuthal shear with range, and this degradation is particularly acute for the 1.8 degree scan (which is the first elevation that does not use the “super-resolution” processing). The variable delta-V actually degrades much less with range (in fact, the observed distribution of values vs. range is almost flat). So, there may be potential to use this variable preferentially at greater distances from the radar. However, we find that azimuthal shear performs better than delta-V in the 0-60 km range bin.

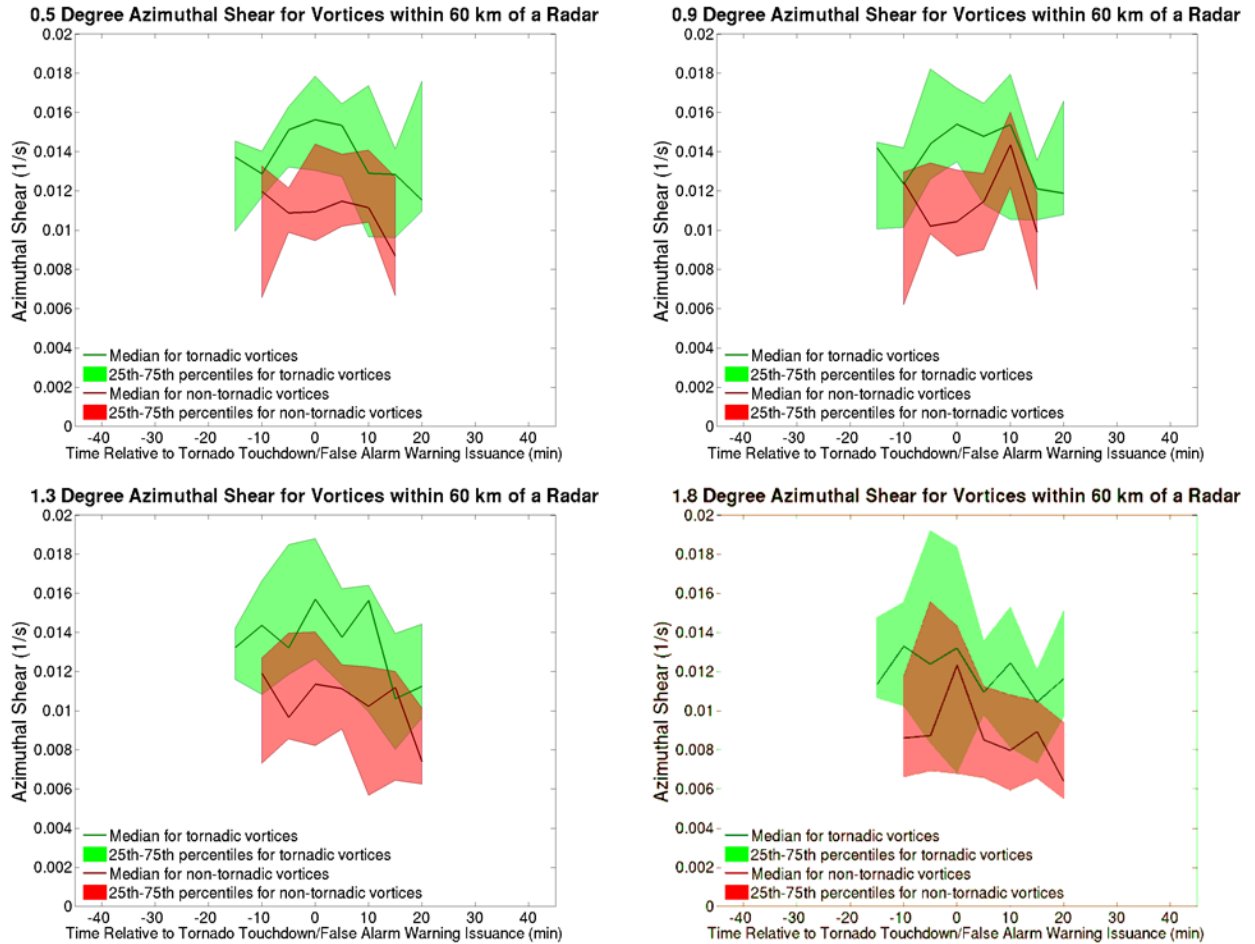


Figure 1.11: Same as Figure 1.9 except only for tracked QLCSs (including 17 tornadic and 12 non-tornadic vortices).

Given the inherent limitations of using velocity products at longer ranges from the radar, the reflectivity climatology was undertaken with the hope that forecasters could still gain some skill on storms whose velocity fields were poorly resolved (or range folded). The reflectivity signatures were compiled by reviewing all four of the lowest elevation scans during the lifetime of each tracked vortex (both tornadic and non-tornadic). After a first pass through the vortices in which common signatures were identified and named, a second pass through the dataset was used to count and catalog the occurrence of each. Unfortunately, there does not appear to be an obvious “smoking gun” among the reflectivity signatures (Table 1.2). Features that our regional collaborating WFOs have described as skillful (e.g. hook echoes, rear inflow notches) are indeed commonly associated with tornadoes, but they are associated with non-tornadic vortices *just as frequently*. Perhaps the most promising sign is that the three QLCS signatures (bottom 3 rows of Table 1.2) are indeed associated with tornadoes much more frequently than non-tornadic vortices. However, even in the most frequently observed QLCS signature (the forward inflow notch) was missing in 55% of QLCS tornadoes, suggesting a rather poor probability of detection. In ongoing work we are trying to determine whether some combination of velocity and reflectivity information can be used more effectively than either field in isolation.

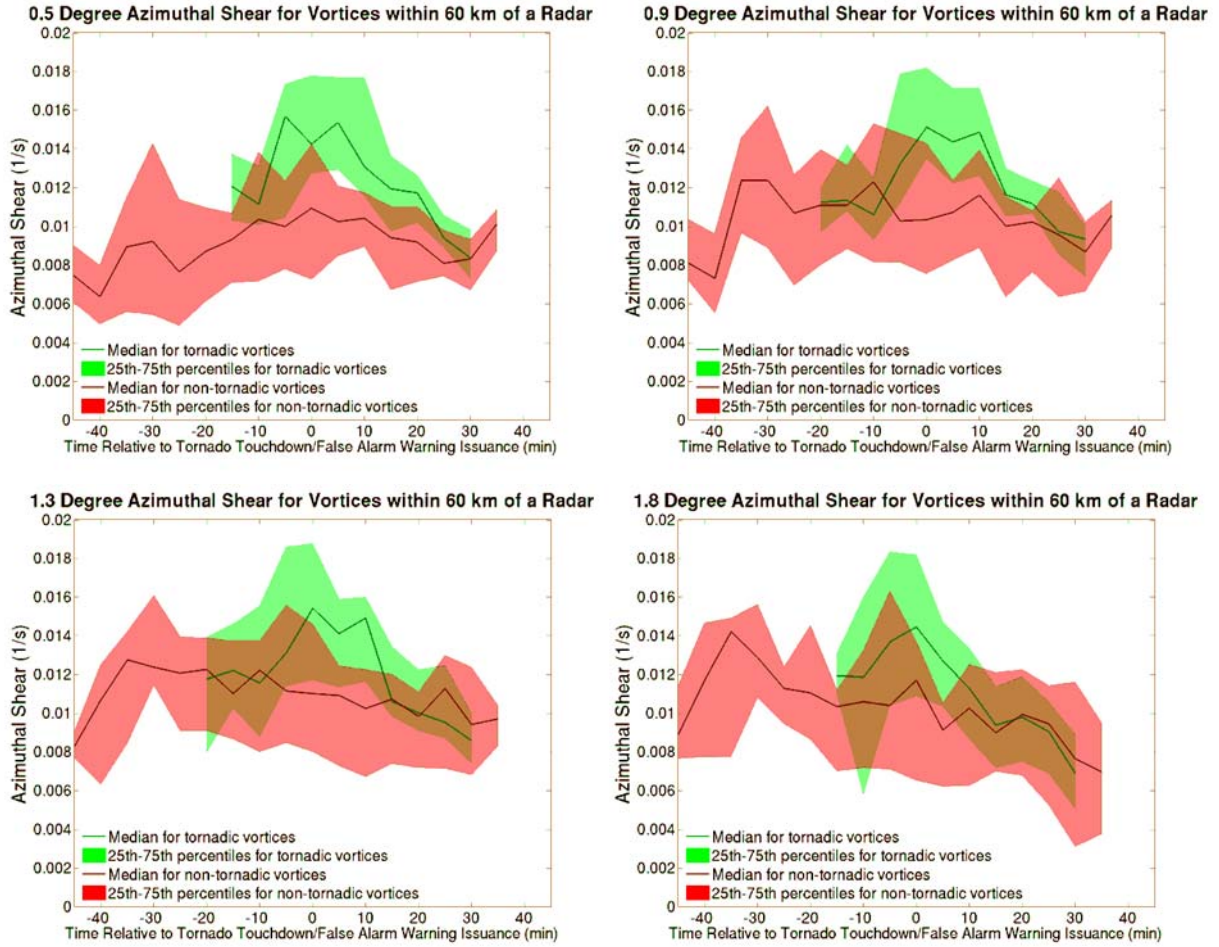


Figure 1.12: Same as Fig. 1.9 except in green are only vortices associated with tornadoes of \geq EF1 intensity (n=19); the null cases (n=29) are identical to those in Fig. 1.9.

	<i>Azimuthal Shear Threshold (1/s)</i>	<i>Tornadic Vortex Median Lifetime (min)</i>	<i>Non-Tornadic Vortex Median Lifetime (min)</i>	<i>Tornadic Vortex Median Lead Time (min)</i>
<i>All vortices</i>	0.006	40	20	15
	0.008	30	10	10
	0.01	20	0	10
	0.012	10	0	5
	0.014	0	0	0
<i>Supercells</i>	0.006	70	50	27.5
	0.008	42.5	30	22.5
	0.01	30	15	17.5
	0.012	15	10	10
	0.014	5	0	5
<i>QLCSs</i>	0.006	22.5	15	5
	0.008	17.5	5	5
	0.01	15	5	5
	0.012	10	5	0
	0.014	5	5	0

Table 1.1: Summary of median vortex properties as a function of the azimuthal shear threshold that is used as a cut-off for identifying them. The full population is shown in the top rows, with only the supercell vortices in the middle rows and only the QLCS vortices in the bottom rows. The lifetimes of the tornadic and non-tornadic vortices are shown separately, and the lead time is shown for the tornadic vortices (this is the amount of time that the tracked vortex exceeded the given azimuthal shear threshold prior to the reported starting time of the tornado).

<i>Reflectivity feature</i>	<i>Tornadic vortices (n=95)</i>	<i>Non-tornadic vortices (n=135)</i>
Hook echo (supercells only)	42 (82 % of sup. tornadoes)	45 (74% of n.t. supercells)
BWER/WER (supercells only)	36 (71% of sup. tornadoes)	52 (85% of n.t. supercells)
Rear inflow notch	50 (53% of tornadoes)	77 (57% of n.t. vortices)
Comma-shaped echo	23 (24% of tornadoes)	25 (19% of n.t. vortices)
Cell Mergers	20 (21% of tornadoes)	33 (24% of n.t. vortices)
Bowing segment	36 (38% of tornadoes)	45 (33% of n.t. vortices)
Forward inflow notch (QLCS only)	18 (45% of QLCS tornadoes)	17 (35% of n.t. QLCSs)
Hook-like echo (QLCS only)	9 (20% of QLCS tornadoes)	4 (8% of n.t. QLCSs)
Broken S (QLCS only)	17 (42% of QLCS tornadoes)	10 (20% of n.t. QLCSs)

Table 1.2: Distributions of reflectivity features subjectively identified for 95 tornadic vortices and 135 non-tornadic vortices tracked for this study. The top two rows are specific to supercells (they were not identified for QLCSs) and the bottom three rows were specific to QLCSs (they were not identified for supercells). For reference, there were 51 tornadic and 61 non-tornadic supercell vortices in the dataset, and there were 40 tornadic and 49 non-tornadic QLCS vortices in the dataset. There were a total of 4 tornadic and 25 non-tornadic vortices classified as “other non-supercell”, which are included in the middle 4 rows.

2.) Winds accompanying landfalling tropical cyclones (Tyner and Aiyyer)

Surface wind gusts are strongly modulated by the state of the planetary boundary layer, including thermal stratification and turbulent processes. The inherent stochasticity of the latter renders the problem of predictability extremely difficult even when high resolution numerical models are deployed. As a result, predictions of tropical cyclone wind speeds have been primarily determined using empirical techniques (e.g., Kaplan and DeMaria 1995; 2001). However, there are numerous gaps in our understanding of spatial and temporal distribution of sustained winds and wind gusts associated with landfalling tropical cyclones. Furthermore, due to variations in synoptic/mesoscale conditions, topography, storm track and storm morphology, empirical wind distribution models developed for one region are not universally applicable. These factors pose a significant impediment to operational forecasters while monitoring and issuing advisories during these catastrophic events. This calls for a development of a dynamical forecasting framework and training of forecast personnel to make optimum use of the same.

Previously, to ensure consistency with the official forecast from the National Hurricane Center (NHC), the process of creating wind and wind gust forecasts in GFE begins with populating wind grids with guidance from the NHC. Forecasters use a smart tool in GFE called the TCMWindTool to ingest and then downscale a tabular text forecast product (TCM) that contains tropical cyclone wind radii at 34 knot, 50 knot, and 64 knot thresholds. These radii are constructed by NHC forecasters to reflect the strongest wind expected in each quadrant [NE, SE, SW, and NW (centered on the storm center and relative to north)]. The wind grids are then constructed according to these radii and the projected path of the storm at 12-24 hour increments. The result is a wind forecast that is not always representative of the true atmosphere. In order to produce a more realistic and accurate forecast, forecasters could potentially use options in the TCMWindTool and other smart tools in GFE to make adjustments to the wind forecast grids. The smart tools allowed forecasters to increase/decrease velocities, add/subtract values to the velocities, multiply/divide by factors, adjust the wind direction, smooth the speed and direction, and more. The original proposal identified significant opportunity for improvement in the existing paradigm of wind forecasting.

a.) NDFD Verification

A systematic analysis of previous National Weather Service forecasts was conducted in the initial phase of this research project. National Digital Forecast Database (NDFD) forecasts were obtained from the National Climatic Data Center (NCDC) for all storms impacting the study region for 2006-2011. Because the study was motivated by wind speeds in true tropical cyclone conditions, remnant storms that made landfall along the Gulf coast and later propagated into the study region were not examined. A list of these storms is shown in Table 2.1.

Ernesto (2006)	Gabrielle (2007)	Cristobal (2008)
Hanna (2008)	Earl (2010)	Irene (2011)

Table 2.1: A list of storms for which an NDFD verification was conducted.

Maximum hourly wind speed forecasts for the duration of the storm were interpolated to a grid matching the available observation stations from the North Carolina Climate Retrieval and Observations Network of the Southeast (CRONOS) database. Due to inherent missing data due to mechanical problems as well as communication failures and power outages, the verification was also conducted using the Hurricane Research Division's (HRD) Real-time Hurricane Wind Analysis System (H*Wind). The limitation of H*Wind analysis are often only created for a short time after landfall. Fig. 2.1 below shows a sample plot for this wind speed verification for Hanna (2008).

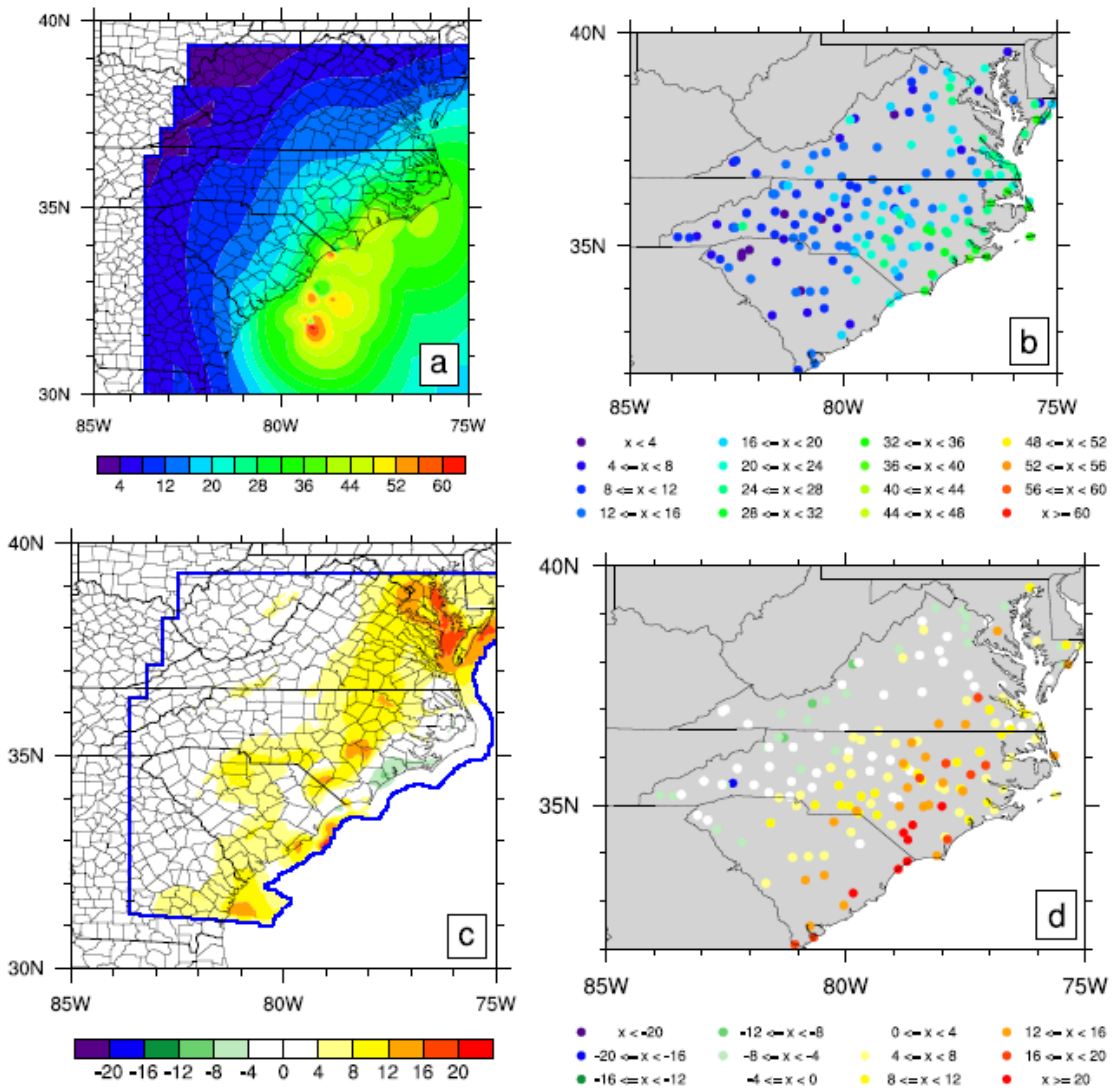


Fig. 2.1: Cristobal (2008) (a) maximum H*Wind analyzed wind speed (kt) over all available analysis times, (b) maximum CRONOS wind speed (kt) station data, (c) wind speed difference between NDFD and H*Wind data (NDFD - H*Wind, kt), and (d) wind speed difference between NDFD and CRONOS data (NDFD - CRONOS, kt).

The NDFD analysis using both CRONOS observations and the H*Wind surface analyses suggested a general over prediction in sustained wind speeds for much of the study region. This over prediction was largest in areas impacted by the strongest wind speeds. Based on the

analysis, forecasters are encouraged to consider using a larger wind decay factor when running the TCMWindTool in order to reduce the over prediction in wind speeds.

b.) Decay Over Land

Currently, the TCMWindTool interpolates the 12-24 hourly wind field forecast from NHC to hourly forecast grids. The tool assumes linear changes in the wind speeds within each 12-24 hour interval. Hourly Rapid-Update Cycle (RUC) analyses with a horizontal grid space of 20 km are available from NCDC for 2002-2011. The RUC analyses were obtained for all landfalling tropical cyclones in the study region during this period of availability in order to evaluate the assumption of linear change. Rapid-Update Cycle (RUC) gridded analyses were acquired for all storms impacting the study region since 2002. The median sustained wind speeds were calculated for various radii from the storm center and for each quadrant.

Consistent with the results of previous work presented in Kaplan and DeMaria (1995), it was determined that the weaker storms had much slower rates of intensity change after making landfall. Because of these slower rates of decay, the assumption of linear decay was not shown to result in significant error for these tropical cyclones. However, two the TCs examined were much more intense and thus subject to higher rates of decay. A temporal analysis of the median sustained wind speeds within the TCM four quadrant 50 kt maximum wind radii is shown for these storms in Fig. 2.2 and Fig. 2.3.

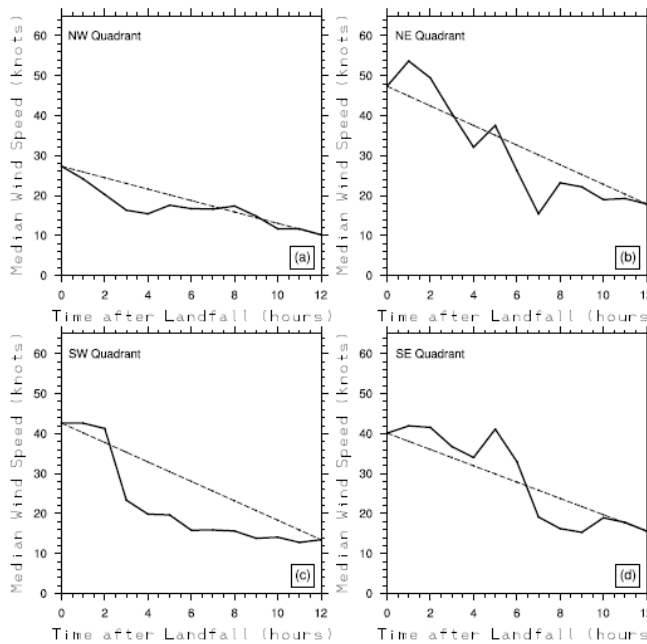


Fig. 2.2. Median RUC analyzed four quadrant wind speed (kt) within the 50 kt maximum wind radius at various times after landfall for Isabel (2003) (solid) along with a 12 hour linear interpolation (dashed). The four quadrants represented are (a) northwest, (b) northeast, (c) southeast, and (d) southwest.

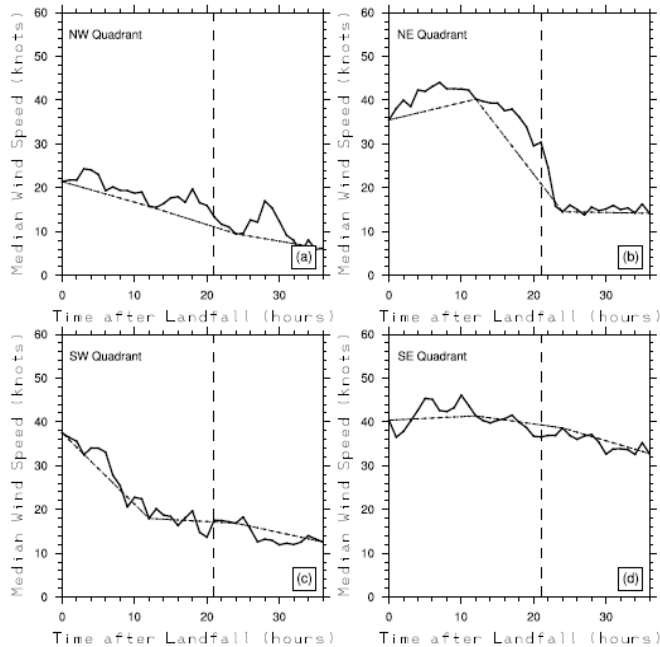


Fig. 2.3. Median RUC analyzed four quadrant wind speed (kt) within the 34 kt maximum wind radius at various times after landfall for Irene (2011) (solid) along with a 12 hour linear interpolation (dashed). The four quadrants represented are (a) northwest, (b) northeast, (c) southeast, and (d) southwest. The vertical lines indicate the approximate time of second landfall for Irene (2011).

As the figures indicate, the tropical cyclones underwent a period of rapid decay in terms of median sustained wind speeds. The period of rapid decay was dependent on the angle of storm approach, with Isabel (2003) taking a more perpendicular approach that led to an earlier period of decay. The decay occurred over a period much shorter than the 12-24 hourly temporal resolution of the NHC wind forecast decay. The linear assumption used in the TCMWindTool to create hourly grids resulted in large error in wind speeds that should be accounted for in future times of tropical cyclone landfall. It is suggested that an alternative automatic interpolation option be added to the TCMWindTool to account for this lack of linear decay after landfall, where forecasters can select the period of rapid decay within the 12 hour raw wind speed forecast guidance provided by the NHC.

c.) Gust Factors

An analysis of gust factors associated with TCs affecting the study region was also conducted. For the gust factor analysis, one-minute Automatic Surface Observing System (ASOS) data was obtained from NCDC for all storms 2000-2011. A list of these storms is shown in Table 2.2.

Kyle (2002)	Isabel (2003)	Charley (2004)	Gaston (2004)	Ernesto (2006)
Barry (2007)	Gabrielle (2007)	Cristobal (2008)	Hanna (2008)	Irene (2011)
Irene (2011)				

Table 2.2: A list of storms impacting the study region 2000-2011.

Gust factors were calculated as the ratio of the wind gust to the sustained wind speed. Gust factors were analyzed based on sustained wind speed as well as wind direction over the study region. Furthermore, a temporal analysis was conducted for each storm at each station to examine how gust factors evolve as the TC passed to complement some of the other analyses (not shown).

Fig 2.3 shows histograms of available one-minute gust factors as a function of wind speed. The results indicate a large variability in the gust factor for weak sustained wind speeds. For wind speed values less than 30 kt, gust factors have a large degree of spread, with values from 1.0-2.2. Furthermore, there are nearly equal frequencies of gust factors of 1.15-1.2, 1.2-1.25, and 1.25-1.3. As the wind speeds increase, the degree of spread in the gust factors decreases and the values converge to lower values. To confirm these results, the standard deviation of the gust factors for the various wind speed bins was calculated. The value for sustained wind speeds less than 30 kt was 0.21, compared to a much smaller value of 0.14 for wind speeds greater than 50 kt. The results suggest the currently used methodology of forecasters using a constant gust factor for all locations within the WFO may be a poor assumption. It is suggested that forecasters consider higher gust factors for locations impacted by weaker sustained wind speeds than locations impacted by stronger tropical cyclone sustained wind speeds. Based on the analysis, a regression equation was developed to account for the change in gust factor as a function of sustained wind speed. This regression equation will be incorporated into the forecast process, as described in the “Research to Operations: WindReductionFactor and GustFactorGrids” section.

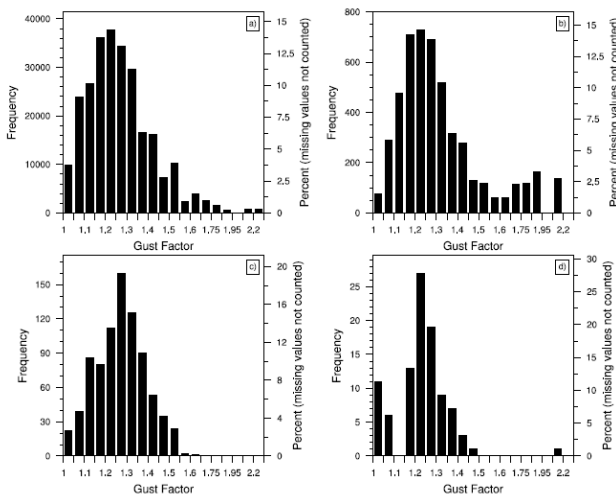


Fig. 2.4: Histograms of gust factors for sustained wind speeds (a) 10-30 kt, (b) 30-40 kt, (c) 40-50 kt, and (d) greater than 50 kt.

In Paulsen and Schroeder (2005), the authors compare gust factors at 10-m averaging periods for tropical cyclone and non-tropical cyclone environments. The results showed that in both environments, gust factors were higher when the wind came from a direction associated with higher upstream surface roughness. Based on this result, it was hypothesized that gust factors at the various ASOS stations with 2-min averaging periods would show a similar bias based on wind direction. In particular, values at coastal locations were expected to be higher for

continental flow with higher associated upstream surface roughness compared to maritime flow. A list of these coastal stations are presented in Table 2.3.

<i>Station ID</i>	<i>Location</i>	<i>Station ID</i>	<i>Location</i>
BWI	Baltimore, MD	SBY	Salisbury, MD
HSE	Cape Hatteras, NC	PHF	Newport News, VA
OXB	Ocean City, MD	ORF	Norfolk, VA
WAL	Wallops Island, VA	EWN	New Bern, NC
ECG	Elizabeth City, NC	MYR	Myrtle Beach, SC
CHS	Charleston, SC	ILM	Wilmington, NC
NHM	Swansboro, NC		

Table 2.3: List of near-coastal ASOS stations for which gust factors were analyzed according to wind direction.

Fig 2.5 shows a histogram of gust factors as a function of wind direction for these coastal sites. The histograms do not indicate a conclusive difference in magnitudes of gust factors based on wind direction. There is a clustering of gust factors near 1.25-1.4, with a gradual spread in other values for all four wind directions. The results suggest that other factors besides upstream surface roughness are important in determining the gust factors. This is consistent with the results presented in Vickery and Skerlj (2005), where local topography and associated surface roughness was found to have a heavy influence on gust factors associated with tropical cyclones.

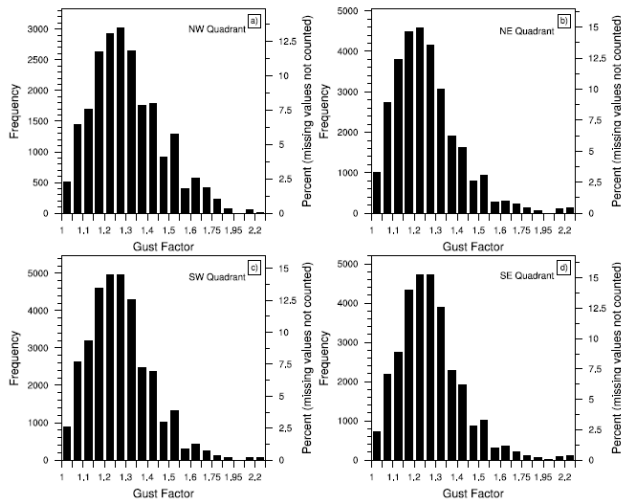


Figure 2.5: Histogram of gust factors for (a) northwesterly, (b) northeasterly, (c) southeasterly, and (d) southwesterly flow.

Based on the results presented in Hsu (2011), it was further hypothesized that locations immediately along the coastline would observe lower gust factors than when the wind was from a direction with a large fetch over land. Hence, for locations right along the coastline, gust factors were analyzed based on wind direction. Fig. 2.6 shows a histogram of gust factors as function of wind direction for Ocean City, Maryland. The histogram suggests a preference in gust factors based on wind direction, with lower gust factors when the wind direction is from the northeast or southeast. As Ocean City is located right along the Atlantic coastline, these wind directions are associated with maritime flow.

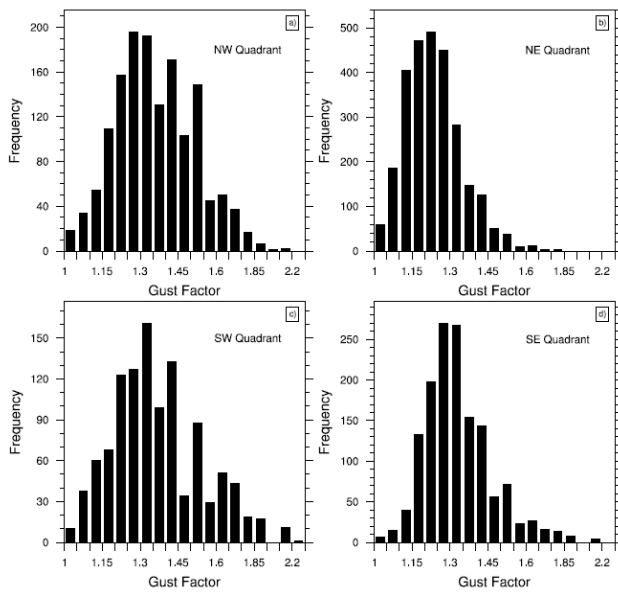


Figure 2.6: Histogram of gust factors at Ocean City, MD for (a) northwesterly, (b) northeasterly, (c) southeasterly, and (d) southwesterly flow.

In contrast, Fig 2.7 shows the gust factor as a function of wind direction for Salisbury, Maryland, a location approximately 50 km inland of Ocean City. For this station, the gust factors do not show a large preference based on wind direction. The results, combined with the previous results, suggest gust factors are largely determined by local surface roughness conditions. For most locations, the local upstream surface roughness is not vastly different based on wind direction. However, for locations immediately adjacent to the coastline, the local upstream surface conditions are inherently different, resulting in a preference for lower gust factors for this maritime flow.

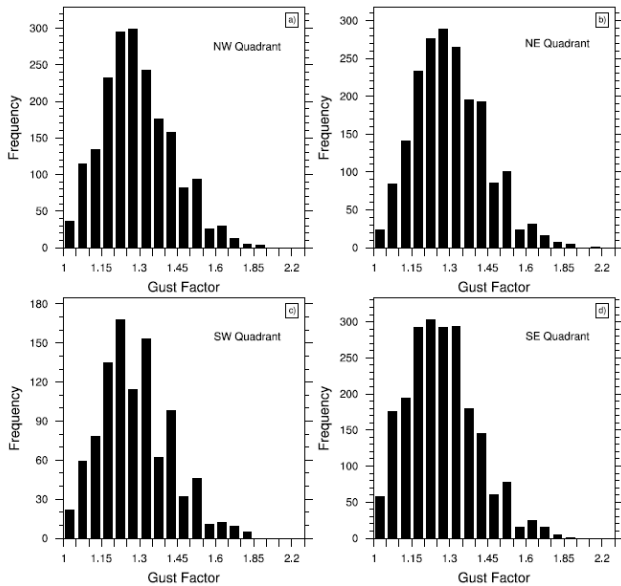


Figure 2.7: Histogram of gust factors at Salisbury City, MD for (a) northwesterly, (b) northeasterly, (c) southeasterly, and (d) southwesterly flow.

d.) Climatologically-based TCM Correction

The TCMWindTool currently uses the Modified Rankine (MR) approach to interpolate the four-quadrant 34, 50, and 64 knot maximum wind radii provided in the NHC TCM product to a grid used by NWS forecasters. The goal of this part of the study was to see if an improvement in the interpolation method could be developed for the TCMWindTool that still maintains the following qualities:

- Is relatively simple to code by the TCMWindTool developers
- Improves rather than replaces the currently used MR approach
- Results in a more collaborative forecast across WFO boundaries
- Retains the original intent of NHC forecasters for the TCMWindTool

H*Wind surface wind speed analyses were obtained from the HRD for 2005-2010 for all Atlantic tropical cyclones. Only analyses for which the tropical cyclone's maximum sustained wind were greater than 64 knots were included in the analysis. A total of 271 analyses met this criteria and hence were used in the study. For each analysis, the MR interpolated wind field was developed using NHC best track data. Error was calculated as the difference between the MR interpolated wind speed and the H*Wind analyzed wind speed as a function of quadrant and distance from storm center. Throughout this analysis, quadrant 1, 2, 3, and 4 refers to the northeast, southeast, southwest, and northwest quadrants respectively. In order to allow for inter-storm comparison, the error for each analysis time was normalized by the NHC best track maximum sustained wind speed. The normalized error was then binned in intervals of 5 km distances from the storm center out to the 34 knot maximum wind radii. Average error was then calculated within these binned distances for each quadrant.

After the average error was calculated, a four degree polynomial fit was applied to the data for each quadrant. Due to the sensitivity in the interpolation method to the radius of maximum winds and the potential errors in the H*Wind analyses near the storm center, data points inside the radius of maximum winds were excluded when developing the error function.

Figure 2.8 shows the 5 km bin-average normalized four quadrant error for the 271 storm analyses examined as well as the four degree polynomial fit. Positive (negative) values indicate interpolated wind speed values larger (smaller) than analyzed. The R-square values are all above .90, indicating a very strong fit to the data. The figure indicates that there are systematic errors as a function of storm quadrant and distance from storm center. In particular, there is a significant positive bias in the interpolated values from the radius of maximum winds to approximately 100-150 km from the storm center. For radii outside 150 km from the storm center, the error is much more minimal, though in general positive. The exception to this is in quadrant 1, where a slight negative bias was present for 150-250 km from the storm center.

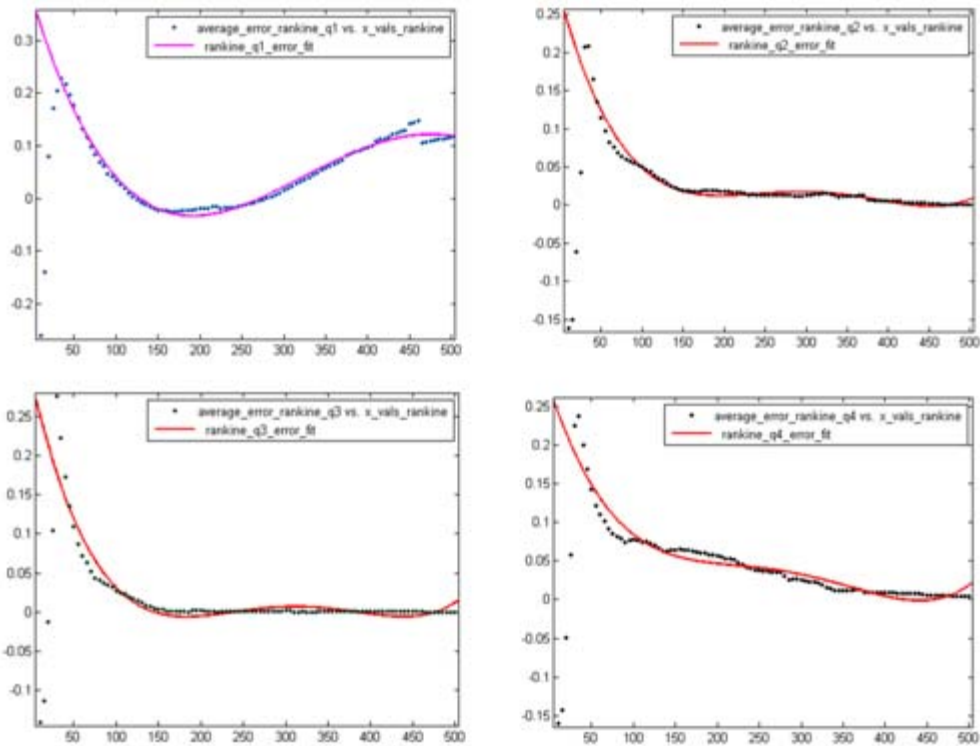


Figure 2.8: 5-km binned normalized average wind speed error (blue dots) and four-degree polynomial fit (solid red line) for (a) northeastern quadrant, (b) southeastern quadrant, (c) southwestern quadrant, and (d) northwestern quadrant.

Outside of the radius of maximum winds, the error functions were subtracted from the four quadrant MR interpolated wind field and a new Modified Rankine Error Function (MREF) interpolated wind field was created. Comparisons were then made between the H*Wind analysis, MR, and MREF interpolated wind speeds for the 271 analyses. The following features were observed by the collaborators in the project

- In the right front quadrant, where the strongest winds typically occur, the MREF winds were typically better in two respects. It shows a quicker decrease in winds just outside the radius of maximum winds, which is often in better agreement with the H*Wind analyses. Furthermore, MREF tends to spread the moderate strength winds further to the northeast than MR, which is consistent with forecaster experiences. As an example, Figure 2.9 shows a comparison of the analysis and interpolated winds for Ike (2008) at 1200 UTC 07 September. It is clear to see the reduction in wind speeds near the radius of maximum winds as well as the increase in moderate wind speeds for the northeast quadrant in MREF, consistent with the H*Wind analysis.

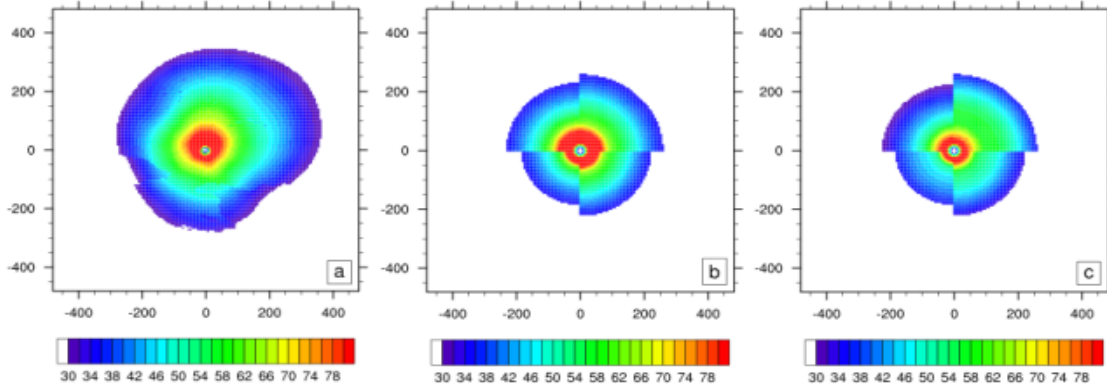


Figure 2.9: (a) H*Wind, (b) MR, and (c) MREF wind speeds (knots) for Ike (2008) at 1200 UTC 07 September

- In the left two quadrants, HREF tends to be more conservative with wind speed magnitudes, which is also consistent with the H*Wind analyses as well as forecaster experiences with storms paralleling the coastline near the Gulf Stream. This can be seen for Ike (2008) at 0000 UTC 13 September in Figure 2.10.

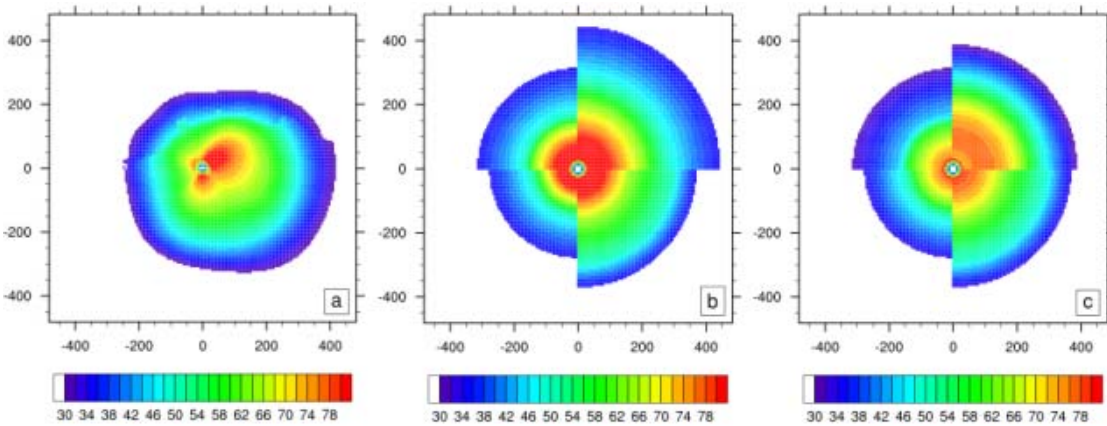


Figure 2.10: (a) H*Wind, (b) MR, and (c) MREF wind speeds (knots) for Ike (2008) at 0000 UTC 13 September

- The currently used MR interpolation method leads to wind speeds too strong for most storms. The fact that the wind speeds are reduced for all quadrants at most distances from the storm center for the MREF winds is a move into the right direction to getting a more accurate base wind field that forecasters can then modify. This can be seen for Dennis (2005) at 0000 UTC 09 July in Figure 2.11.

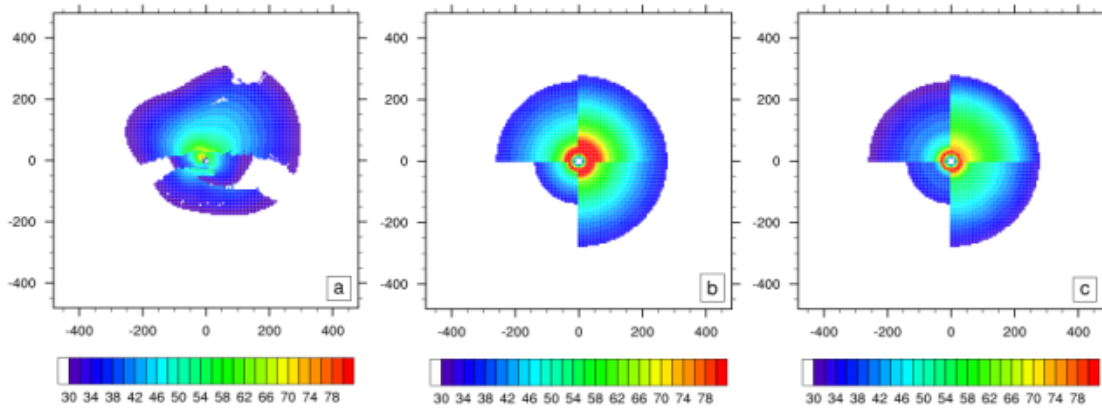


Figure 2.11: (a) H*Wind, (b) MR, and (c) MREF wind speeds (knots) for Dennis (2005) at 0000 UTC 09 July

e.) Research to Operations: Improved Wind Field Interpolation Methods

As described, a climatologically-based correction to the TCM guidance was developed. The inclusion of this correction, MREF, into the TCMWindTool was recommended and approved at the 2013 NOAA Hurricane Meeting in December 2013. Participants from WFOs Raleigh, NC, Wilmington, NC, Morehead City, NC, Wakefield, VA, Charleston, SC, and Miami, FL will test and evaluate the performance of this new MREF during the 2014 Tropical Cyclone Season. Forecasters at four WFOs had an opportunity to test the new wind field interpolation method during Hurricane Arthur (2014) and the results were very encouraging with a consensus that the output “looked realistic” and the integrated tool was “even more efficient than in past years, likely due to the tweaks to the TCMWindTool.” The CSTAR based MREF is available to forecasters within the TCMWindTool as “NC State Bias Correction” as shown in Fig. 2.12

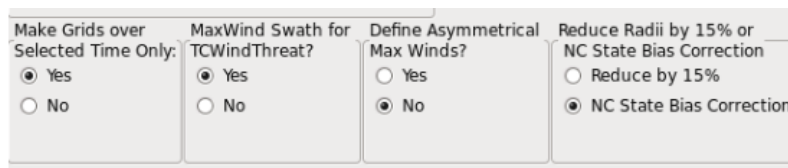


Fig. 2.12: Options for WFOs to use MREF options in the 2014 version of the TCMWindTool.

f.) Research to Operations: Wind ReductionFactor and GustFactor Grids

The results of the study have been used to develop new WindReductionFactor and GustFactor grids. The new grids allow for land reduction and gust factors that vary spatially and temporally across a Graphical Forecast Editor (GFE) domain. It is believed that these new grids will add science to the forecasting process, improve on forecast consistency from forecaster to forecaster and among neighboring WFOs, and result in a more efficient process to create wind and wind gust grids. The WindReductionFactor and GustFactor grids were operationally tested by three WFOs with Tropical Cyclone Andrea (2013) and with four WFOs with Hurricane Arthur (2014). Feedback from forecasters during Arthur was very positive with forecasters noting the new process “included more science”, “produced realistic output”, and “end result was ideal”. Additional testing is planned during the remainder of the 2014 tropical

cyclone season. Images of the use WindReductionFactor and GustFactor tools are shown in Fig. 2.13 below.

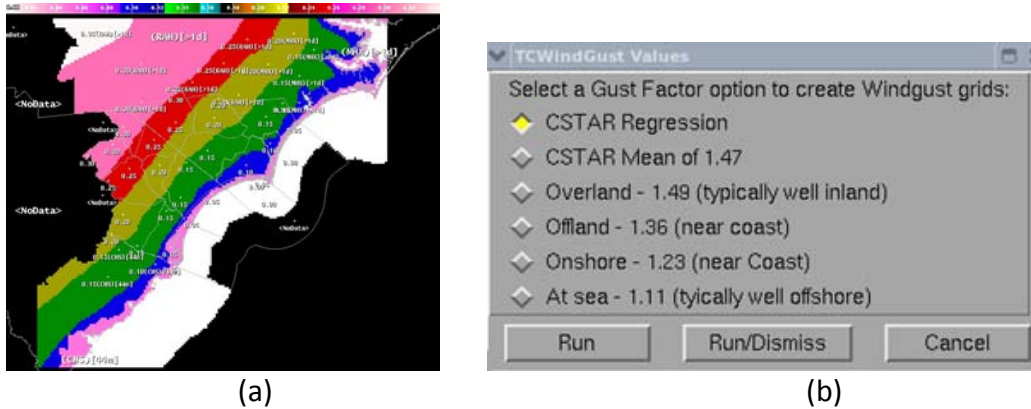


Fig. 2.13: Sample use of (a) WindReductionFactor grid and (b) GustFactor options for WFOs to test for the upcoming tropical cyclone season.

h.) Future Work and Research Summary

The results of the work aimed at improving tropical cyclone sustained wind speed and gust forecasts in the study region were summarized in a paper submitted to Weather and Forecasting in October, 2013 (Tyner et al. 2014 – see references). The paper has since then been revised, following the constructive comments of three anonymous reviewers. The revised manuscript was submitted to the editor in April, 2014. Some key earlier results include:

- Tropical cyclones making landfall in the southeastern US often undergo a period rapid decay in terms of sustained wind speeds. The period of rapid decay typically depends on the angle of storm approach with respect to the coastline. The decay occurs over a period much smaller than the 12-24 hourly temporal resolution of the NHC wind forecast data. The linear assumption used in the TCMWindTool to create hourly grids likely results in significant error in wind speeds that should be accounted for.
- The NDFD verification using both the observations from the CRONOS data network and the H*Wind surface analyses suggest a general over prediction in sustained wind speeds for much of the study region. Forecasters are encouraged to consider using larger land reduction factors in the TCMWindTool and to collaborate among Weather Forecasting Offices (WFOs) on these land reduction factors to improve the sustained wind speed forecasts for future TCs.
- Gust factors are highly variable at lower sustained wind speeds. The variability in the gust factors significantly decreases as the sustained wind speeds increase; furthermore, these gust factors nearly asymptotically decay to values near 1.1-1.2 for sustained wind speeds above 40 knots. Although there was no general conclusive bias in gust factors based on wind direction, locations near the immediate coastline displayed lower gust factors when the flow was from the maritime environment. Forecasters should consider

the sustained wind speed, wind direction, boundary layer stability, and local topographic effects when choosing a gust factor to create wind gust forecasts.

The newly developed WindReductionFactor and GustFactor grids have been developed and distributed to the local Weather Forecasting Offices of Raleigh, Wilmington, and Morehead City, NC, Wakefield VA, Charleston SC, and Miami FL. The tools are undergoing further testing during the 2014 tropical cyclone season before potential distribution to other Weather Forecasting Offices in future seasons. These new fields are designed to improve forecast consistency between forecasters and among neighboring WFOs, and provide a more efficient process to create wind and wind gust grids.

The motion to include the climatologically-based bias correction, known as the Modified Rankine Error Function (MREF), into the TCMWindTool was approved at the December 2013 NOAA Hurricane Meeting. The MREF has been coded and implemented into the TCMWindTool. It will be tested by WFOs Raleigh, Wilmington, Morehead City, Wakefield, Charleston, and Miami.

As a follow up to the CSTAR tropical cyclone wind work, the characteristics of the landfalling hurricane boundary layer have been examined using the Weather Research and Forecasting (WRF) Model. The work is supported by National Science Foundation Grant ATM-0847323. Since version 3 of WRF, a large-eddy-simulation (LES) option has been available for the planetary boundary layer. Select simulations were conducted for Irene (2011) using two popular planetary boundary layer schemes in the mesoscale domains: the Yonsei University (YSU) non-local scheme and the Mellor-Yamada-Janjic (MYJ) local scheme. The preliminary results of the work suggest the simulation conducted using the YSU scheme produced a stronger tropical cyclone, likely attributed to the presence of localized strong areas of convection from the outer rain bands of the tropical cyclone. An examination of the boundary layers within the LES domains showed the presence of large-eddy circulations (LECs) within the eyewall. The LECs were limited in vertical extent to the top of the boundary layer. The horizontal sizes of the LECs were different between the simulations, with the LECs in the MYJ simulation having a broader range of sizes than in the YSU simulation. The preliminary results suggest the characteristics of the simulated hurricane boundary layer within the LES domain are sensitive to the planetary boundary layer scheme chosen for the outer domains. Further sensitivity studies will continue to examine the characteristics of these simulated LECs in the boundary layer.

3.) Inland TC precipitation (Dale, Gordon and Lackmann)

This research component features two broad sub-problems, including: (a) tropical cyclone initial condition representation in NWP models, (b) quantitative precipitation forecasting with landfalling TCs. The latter can further be sub-divided into TC-boundary interaction as a QPF challenge, the development and influence of cold-air damming during a landfalling TC, and predecessor rain events (PREs).

(a) Tropical cyclone initial conditions

A prerequisite to accurate numerical prediction of inland TC impacts is an adequate model initial condition for the TC itself. Unfortunately, there are difficult challenges to overcome in this regard. As of the time that the original proposal was written, the GFS and NAM initial analyses often include initial TC representations that are too weak, in part due to resolution, but also because the data assimilation systems used to generate the analyses are not optimally designed for TC initialization. The GFS data assimilation (DA) system was upgraded in 2012, with drastic improvements in model initial conditions, especially with regard to tropical cyclones. Still, for TCs that are intense as they approach land, “standard issue” operational initial conditions will not be adequate. Due to the upgrade in the GFS DA system, and also due to the departure of Dr. Etherton from RENCi, the project focus emphasis shifted towards TC QPF during the latter portion of the funding period. As a summary of the TC DA problem, Dr. Lackmann presented an in-depth webinar on 5 July 2012 detailing how the GFS and other NCEP operational models initialize tropical cyclones, with an emphasis on operational aspects. A summary of the DA aspect of the CSTAR work done during years 1 and 2 of the project will follow.

One available strategy that has been used with some success in experimental systems is to include a bogus vortex, available from the GFDL hurricane model (e.g., Kurihara et al. 1993; Davis et al. 2008). By inserting a synthetic vortex with strength comparable to the observed TC at the time, model forecasts no longer have to play “catch up” to obtain a storm that is of sufficient intensity upon landfall. A recent study of Hurricane Isabel has demonstrated some added value in the use of the GFDL vortex in this case (Lin et al. 2010). However, as noted in that study as well as CSTAR research with Hurricane Ike, even with the inclusion of a bogus vortex the model is not able to capture the effects of initial asymmetries such as outer spiral rainbands. These features are important producers of high-impact weather in their own right, and may also factor significantly in the dynamics of the storm itself (e.g., Hill and Lackmann 2009).

Former M.S. student Briana Gordon worked with a quasi-operational WRF-based hurricane prediction system, HUR-NC, to analyze TC structure in three different tropical cyclone initial condition options, and to examine how TC structures evolve from these initial conditions when integrated through time. HUR-NC, run at RENCi, featured a parent domain with 27-km grid spacing and two storm-following one-way inner nests with 9-km and 3-km grid length. Briana examined one strong case (Hurricane Ike, 2008) and one weak case (Tropical Storm Erika, 2009), in order to see how changing the initial condition affects the forecast in these different scenarios.

For the 2008, 2009, and 2010 Atlantic hurricane seasons, HUR-NC ran in real time from July through November, allowing evaluation over a series of TC cases. Subjective verification indicated that this modeling system exhibited considerable skill for both track and intensity even when using unmodified (no bogus vortex) GFS 0.5 degree initial condition data, but for runs in which a TC is strong at the time of initialization there is a substantial intensity error, with the initial intensity up to 60 mb too weak in some cases. Clearly, such dynamical forecasts would not be useful for the prediction of inland impacts. In an effort to more closely estimate storm structure and intensity at the initial time, HUR-NC was re-run for Hurricane Ike and Tropical Storm Erika using the GFDL bogus vortex at the initial time. A method for blending the GFDL vortex with the GFS initial conditions was obtained from Dr. Bob Hart (Florida State University).

For Ike, which was already a mature storm when we initialized the model for the test runs considered here, the bogus vortex did improve the intensity forecast for the first 24 hours of the forecast, but the GFS-only model run behaved comparably with the GFDL/GFS merged model run beyond that lead time (not shown). For the run of 12 UTC 10 September 2008 (Fig. 3.1), the GFDL vortex featured a central pressure of 964 mb, compared to 980 mb in the GFS-only initial conditions. The NHC best track lists the central pressure of Ike at 959 mb at that time.

Differences in the potential vorticity structure of the initial TC are striking, with the GFDL vortex characterized by a very strong PV tower, including a maximum near the 400-mb level (Fig. 3.2b); the GFS-only initial condition exhibits a weaker and more diffuse PV tower that is approximately 1/3 as strong (Fig. 3.2a).

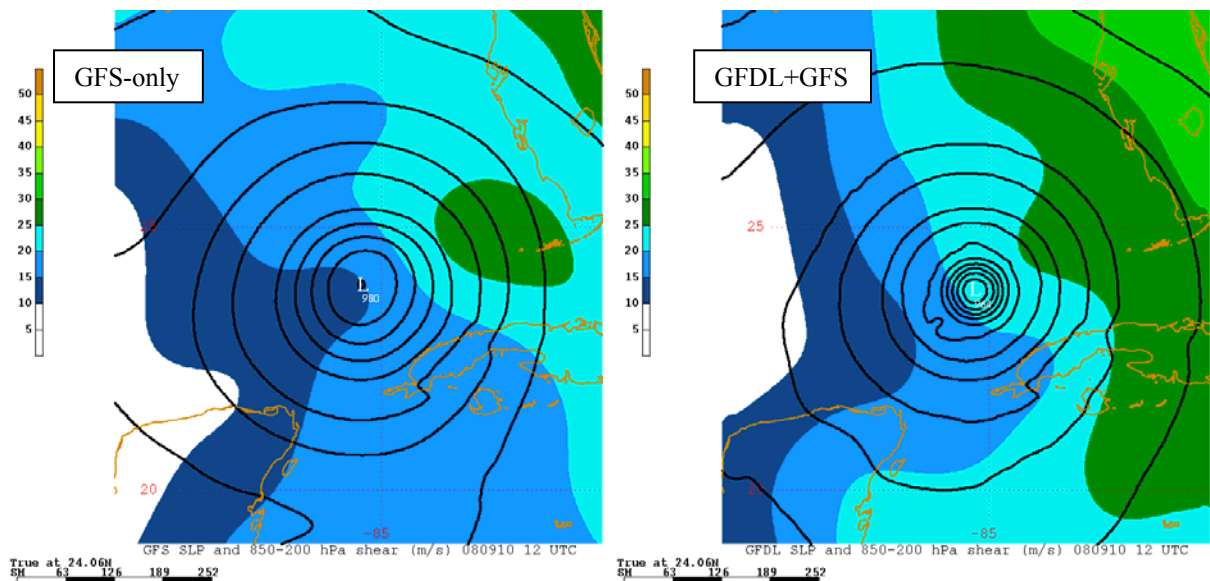


Figure 3.1. Hurricane Ike run of 12 UTC 10 September 2008. Initial sea level pressure (contour interval 4 mb, central pressure indicated in white text) and 850-200-hPa shear (shaded) for (a) GFS-only initial conditions, and (b) GFDL+GFS initial conditions.

In order to show a contrasting case featuring a TC that is weak at the initial time, we present Tropical Storm Erika at 00 UTC 2 September 2009. The NHC best track lists Erika at 1004

mb at this time, compared to 1009 mb in the GFS-only initial condition (Fig. 3.3a) and 1001 mb in the GFDL+GFS initial conditions (Fig. 3.3b).

In this case, the forecast was not improved by the bogus vortex, probably due to the fact that the robust bogus vortex is not a good proxy for a weak, sheared tropical storm such as Erika. In fact, we hypothesize that the addition of the bogus vortex may have artificially strengthened the storm to the point where it was unrealistically resistant to vertical wind shear. The PV cross sections shown in Fig. 3.4 document a highly robust structure in the GFDL+GFS initial conditions, which is likely too strong at upper levels.

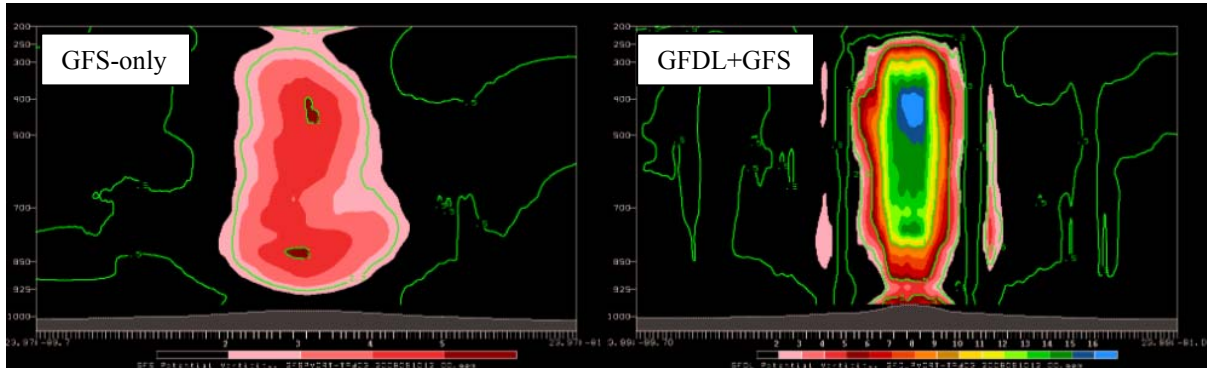


Figure 3.2. Storm-relative cross sections of potential vorticity corresponding to the analyses shown in Fig. 1 for (a) the GFS-only initial conditions, and (b) the GFDL+GFS initial conditions.

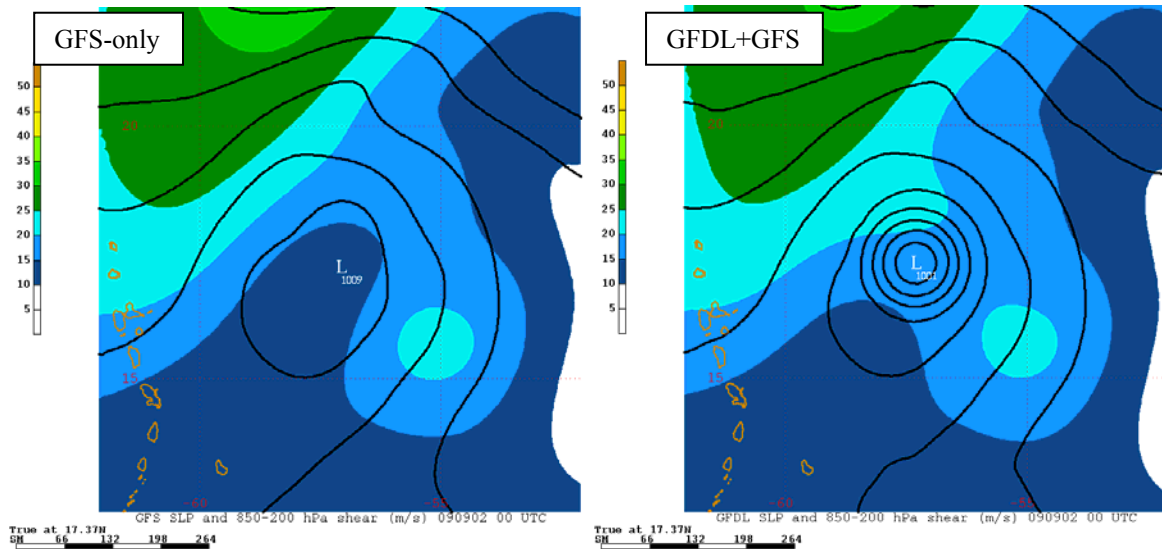


Figure 3.3. As in Fig. 3.1, except for Tropical Storm Erika at 00 UTC 2 September 2009.

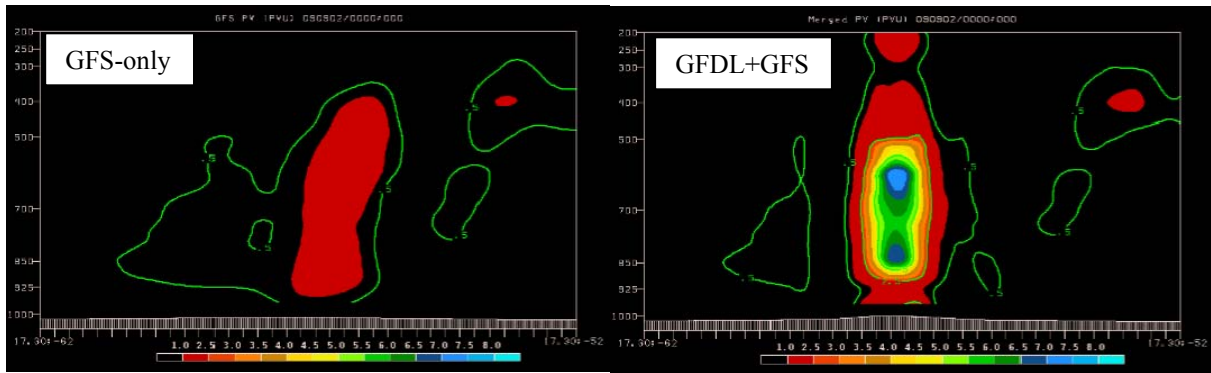


Figure 3.4. As in Fig. 3.2, except for Erika at 00 UTC 2 September 2009.

Given the limitations in bogus vortex initialization, Dr. Etherton, prior to his departure from RENCi, set up a prototype system for Briana Gordon to use in experimental generation of tropical cyclone initial conditions. This system utilizes a 24-member ensemble of short-term (6-h) WRF runs as a component of the data assimilation (DA) process. The critical aspect of DA is devising a means of optimally weighting observations versus the background, or first guess field. In the hybrid system developed here, the ensemble mean is used for the first guess, and the ensemble spread is used in defining the background error covariance matrix, which weights observations and first guess. Additional observations, in the form of dropsondes from Air Force hurricane recon flights obtained in decoded form from www.tropicalatlantic.com, were assimilated using the WRF-Var assimilation system.

The case selected for testing was Hurricane Earl (2010). The test model runs were conducted for a time when Earl was a strong hurricane at the time of model initialization, and during a time period when it was threatening the U.S. East Coast. The addition of recon dropsonde data in conjunction with the ensemble enabled the development of an initial condition that improved upon both the standard-issue GFS as well as the GFDL bogus vortex initial conditions.

Plots comparing the potential vorticity for four different model initial conditions are shown below (Fig. 3.5). Clearly, the addition of the bogus vortex adds a very strong and narrow PV maximum to the initial condition that differs from the three other initial conditions. The corresponding sea level pressure and 10-m wind fields for these four initial conditions are shown in Fig. 3.6. The minimum sea level pressure in each analysis is consistent with the strength of the PV towers shown in Fig. 3.1, that is, the GFDL initial condition is stronger, and closer to observations than are the other analyses. The best-track value of central pressure for Earl at this time is 940 hPa, whereas the GFS featured 981 hPa, the GFDL 949 hPa, the ensemble without additional observations had 966 hPa, and the ensemble with dropsondes exhibited a pressure of 968 hPa.

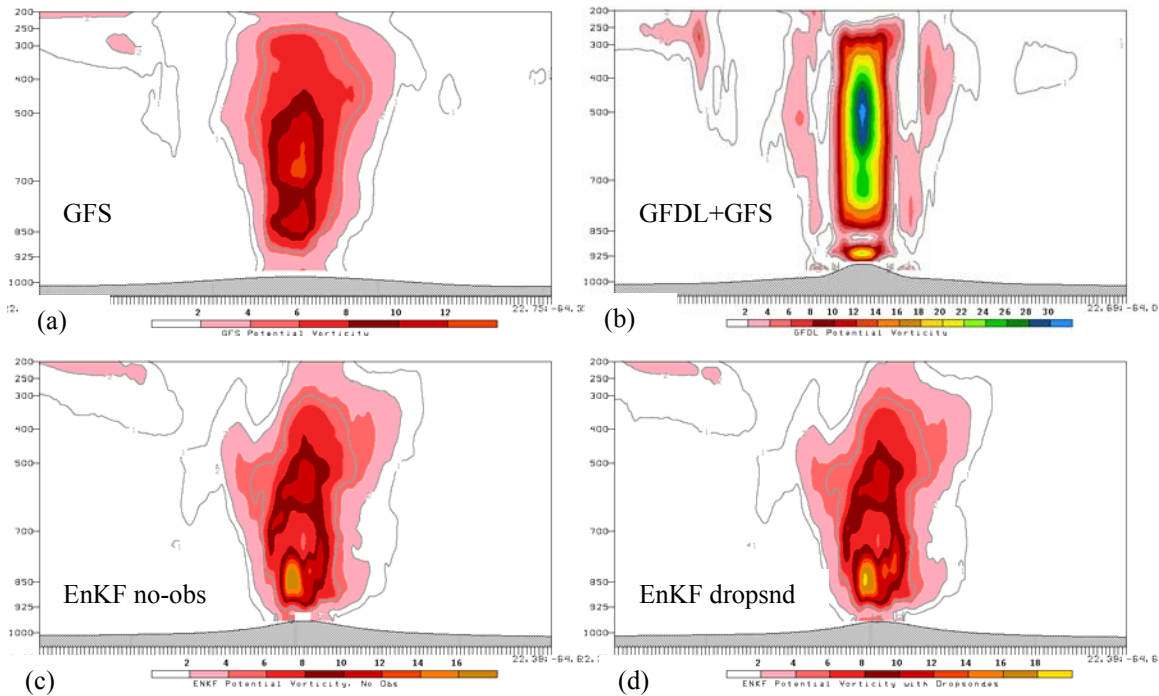


Figure 3.5. Comparison of initial conditions for Hurricane Earl run of 00 UTC 1 September 2010. Cross sections of potential vorticity (PVU, shaded as in legend at bottom of panels): (a) GFS-only initial conditions, (b) as in (a) except for GFS with GFDL bogus vortex; (c) ensemble only with no additional observations; (d) ensemble with recon dropsonde observations assimilated.

The pattern of 10-m wind speeds is generally strongest in the northeast quadrant of Earl, consistent with the northwestward motion of the storm at this time. The only initial condition not to reflect this is the EnKF without additional observations, which exhibits a maximum in the northwest quadrant of the system (Fig. 3.6c). While the two ensemble-based initial conditions are still too weak relative to observations, they represent a significant improvement over the GFS-only initial condition.

The difficulty of obtaining accurate initial conditions for TCs that are strong (e.g., central pressure < 970 mb) at the time of initialization is not easily overcome. The EnKF technique tested here shows promise, but the potential benefit is not realized in the short-term experiment conducted here. Unfortunately, due to the departure of Dr. Etherton from RENCi, and due to the failure of a major disk drive at RENCi, we were not able to continue testing of this system. Additionally, a presentation sharing our lessons learned about how operational models are currently initialized for tropical cyclones was prepared and presented as a part of seasonal familiarization material prior to the 2012 Atlantic hurricane season.

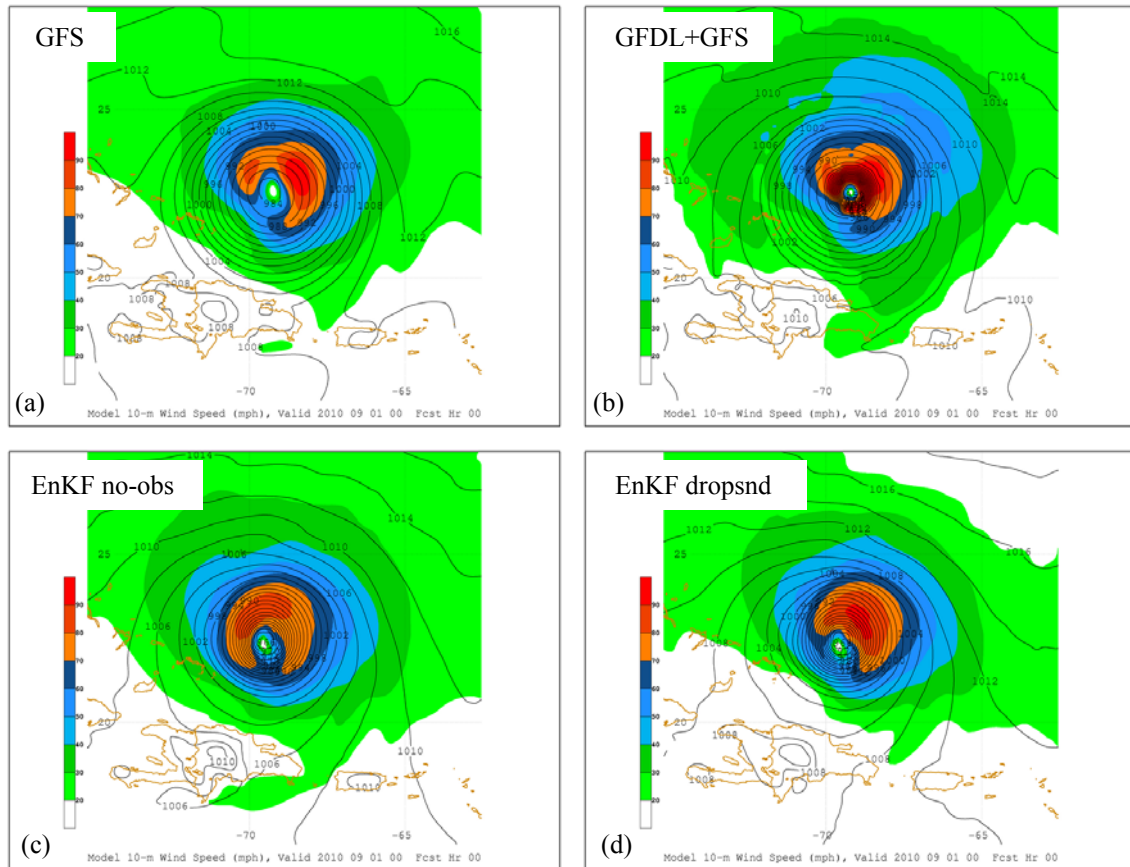


Figure 3.6. As in Fig. 3.1, except showing sea level pressure (contour interval 4 hPa) and 10-m wind speed (kt, shaded as in legend at left of panel). The relative location of the four panels is as in Fig. 3.1.

b.) Tropical cyclone QPF

Graduate student Jordan Dale joined the project to head up the TC-QPF problem. Based on collaborations with NWS CIs, a survey was conducted, and a list of candidate TC events was developed for in-depth study. The initial focus was to elucidate the role of frontal boundaries in influencing TC QPF. From a list of 54 tropical cyclones (TCs), the following criteria were used to select candidate cases:

- Events must take place after the year 2000 to allow for more complete data and better forecaster recollection;
- The storm center was required to move over the Carolinas and/or Virginia, or close to the coast;
- Rainfall must exceed 6 inches over the Carolinas and/or Virginia.

In all of the cases identified, there was a frontal boundary of some type in the vicinity of the storm, and typically these were synoptic-scale features analyzed on archived NCEP/HPC surface analyses. A Google document was then created and shared with field offices and other collaborators to solicit input on each of the identified storms. Input included forecast challenges, errors or successes, as well as insight or opinions on how precipitation was altered by any boundary interactions during the event. WFOs then took a rough inventory of any

archived data they had for the list of cases. Based on the available data, forecaster comments, and impacts (damage, fatalities) for each storm, the TC QPF group then selected Tropical Storm Ernesto from 2006 (Fig. 3.7) as an initial case for further study. Ernesto had a fairly strong frontal boundary (for the season), making it a good comparison case versus the weaker, in-situ boundary present in Tropical Storm Hanna (studied previously by the group).

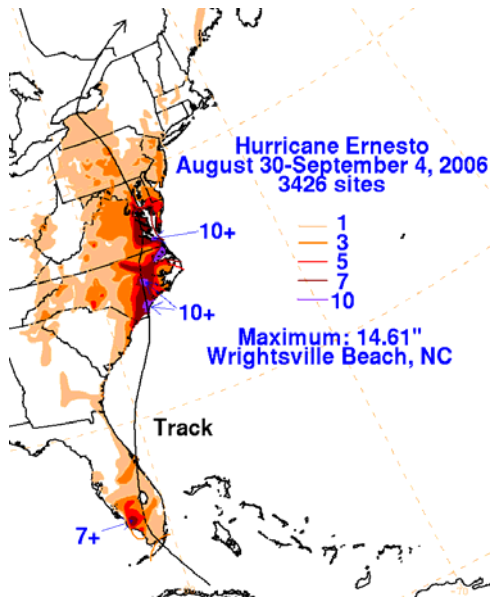


Fig. 3.7. Storm total precipitation for the period 30 August to 4 September 2006 (HPC).

Before Ernesto made its second landfall in North Carolina, an MCS developed in NC and VA along a cold front, which was pushing through the SE US on 30 August. The Predecessor Rain Event (PRE) criteria of Galarneau et al. (2010) are: 1) Radar reflectivity must exceed 35 dBZ for at least 6 hours, 2) Total rainfall must exceed 100 mm (4") in 24 hours, 3) A clear separation must exist between the PRE and TC rain shields, and 4) Deep tropical moisture from the TC must be advected into the vicinity of the PRE. Analysis indicates that the MCS over the study region on 30 August 2006 met all these criteria. Furthermore, Galarneau et al. (2010) classified the MCS preceding Ernesto as a PRE.

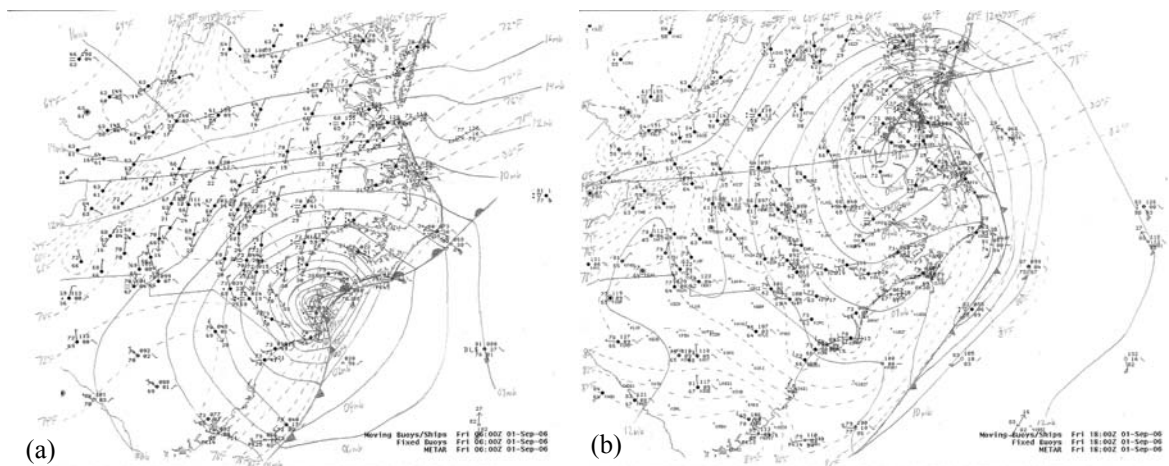


Fig. 3.8. Manual analyses from Ernesto event: (a) 0600 UTC, and (b) 1800 UTC 1 September 2006.

After the MCS/PRE dissipated, the cold front stalled along the coast around 0600Z 31 August. As Ernesto approached the coastline, the coastal front strengthened and became entrained into the circulation between 0000Z and 0600Z 1 September. As Ernesto moved inland, it began transitioning into an extratropical cyclone with a more traditional frontal structure developing by 0600Z 1 September (Fig. 3.8a). An occluded type frontal structure evidently developed by 1800Z 1 September as Ernesto moved into Virginia (Fig. 3.8b, 3.9b).

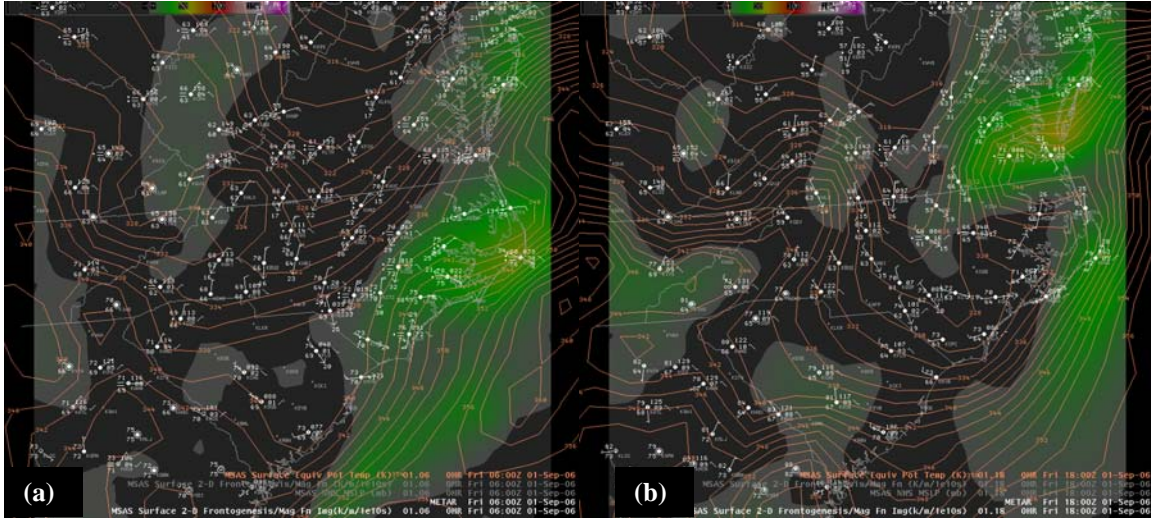


Fig. 3.9. MSAS surface 2-D frontogenesis (fill) and equivalent potential temperature (contour): (a) 0600 UTC, and (b) 1800 UTC 1 September 2006.

We speculate that the presence of a frontal boundary may have provided enhanced forcing for lift, particularly to the east of the TC center where a moist southerly flow was impinging on the frontal boundary. In the vicinity of frontal lifting nearest the TC center where the circulation and resultant lifting was strongest, a region of enhanced radar reflectivity NE of the TC center (Fig. 3.10a,b) led to a swath of extremely heavy rainfall producing storm total accumulations in excess of 10 inches through parts of eastern North Carolina and Virginia (Fig. 3.7).

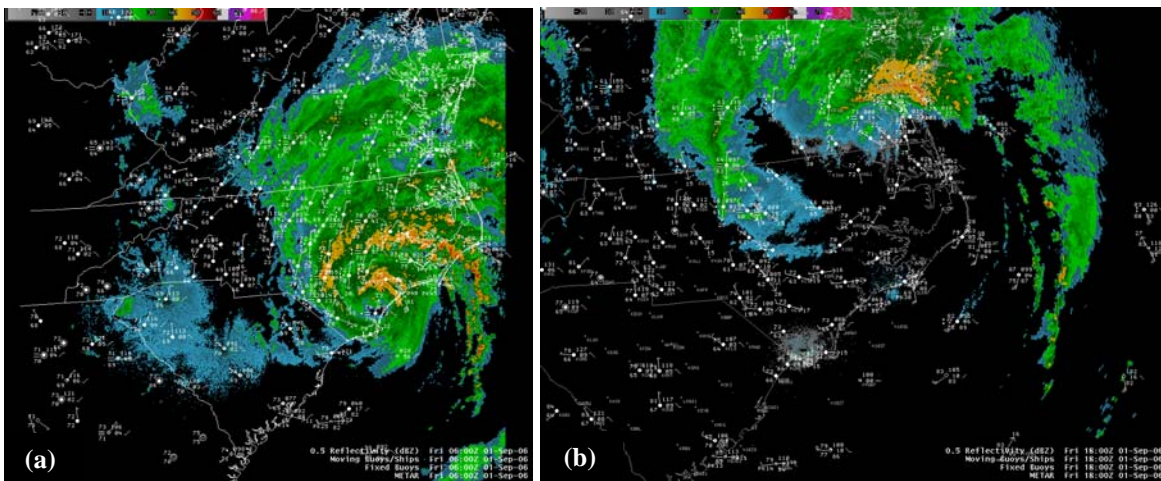


Fig. 3.10. Composite radar reflectivity, (a) 0600 UTC, and (b) 1800 UTC 1 September 2006.

The manual analyses, based on observational data sources, were corroborated by gridded analyses to arrive at a consistent set of “ground truth” analyses (e.g. Fig. 3.11). The next step was to examine predictability issues. In addition to the PRE classification for this event, the analyses also indicated that a weak cold-air damming (CAD) event became established over NC prior to Ernesto’s landfall. Based on the analyses, predictability questions included: (i) did the PRE alter the pre-landfall environment sufficiently to affect subsequent TC QPF (e.g., by affecting mesoscale boundary development, intensity, and position)? (ii) Was the PRE related to the weak CAD event? (iii) Were the lack of PRE and CAD representation in model forecasts related to the westward post-landfall track bias for Ernesto (in model and NHC forecasts)? An ensemble modeling strategy was adopted in order to address these questions. During summer and early fall 2012, Jordan Dale ran the WRF-ARW model with a variety of physics selections and with different initial condition data and times.

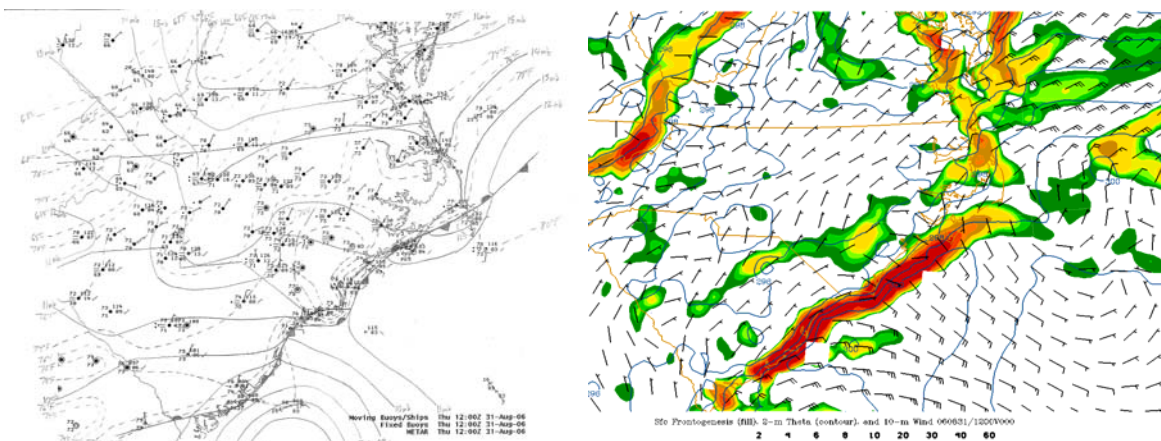


Figure 3.11. Comparison of manual temperature, sea-level pressure, and frontal analysis (a) with objective computation of 2-D frontogenesis using RUC gridded analyses for 12 UTC 31 August 2006.

Control simulations with WRF utilized a nested-grid approach (Fig. 3.12). The model was configured with 47 vertical levels, and with a 36-12-4 km grid length for the outer, middle, and innermost domains, respectively. Initial conditions were obtained from both GFS and ECMWF analyses.



Figure 3.12. WRF domains used for Ernesto simulations: outer domain features 36-km grid spacing, with a 12-km and 4-km middle and innermost domain grid length, respectively.

The outer-domain WRF forecasts and simulations exhibited limited representation of the PRE, which formed along a synoptic front (Fig. 3.13), although subsequently, radar comparison indicates that the model was able to capture the TC precipitation shield to a better extent (Fig. 3.14).

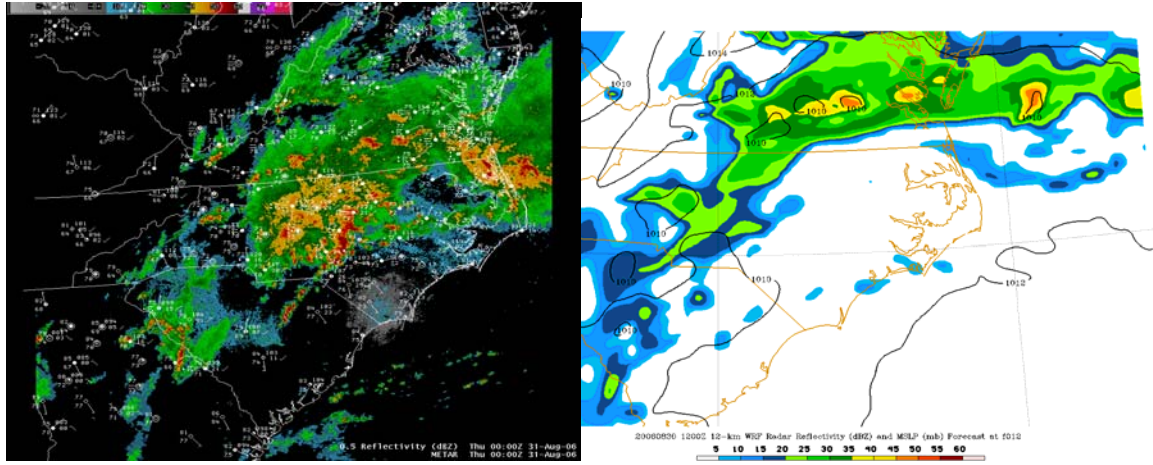


Figure 3.13. Base-level reflectivity (left) and WRF simulated composite reflectivity (right) for 00 UTC 31 August 2006.

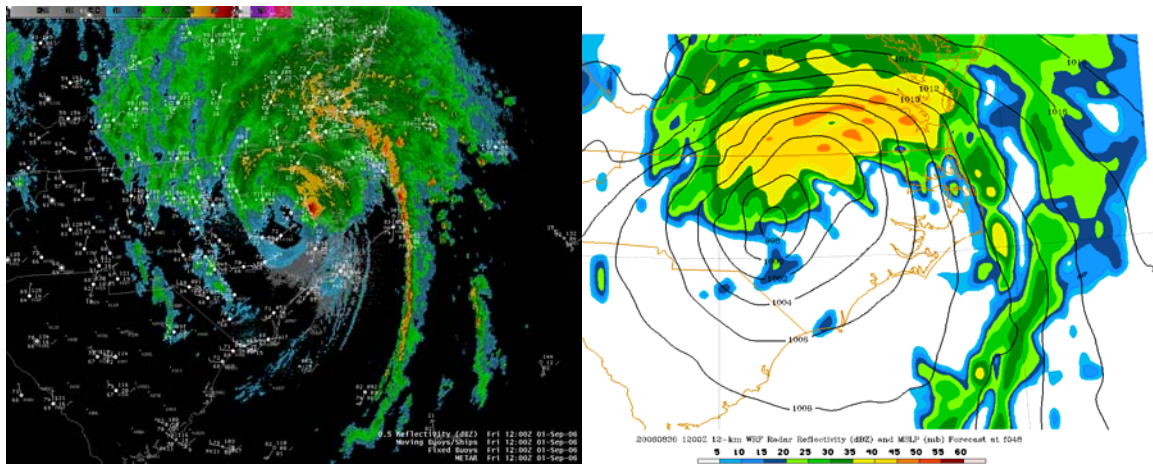


Figure 3.14. As in Fig. 3.13, except for 12 UTC 1 September 2006.

Comparison of QPF from the WRF control simulation with Stage-IV quantitative precipitation analyses (QPE) demonstrate that the model generated realistic QPF, but that the axis of heaviest precipitation was shifted westward relative to the QPE (Fig. 3.15). This is consistent with the westward track bias that was evident both in operational forecasts at the time and in numerical forecasts and simulations (Fig. 3.16).

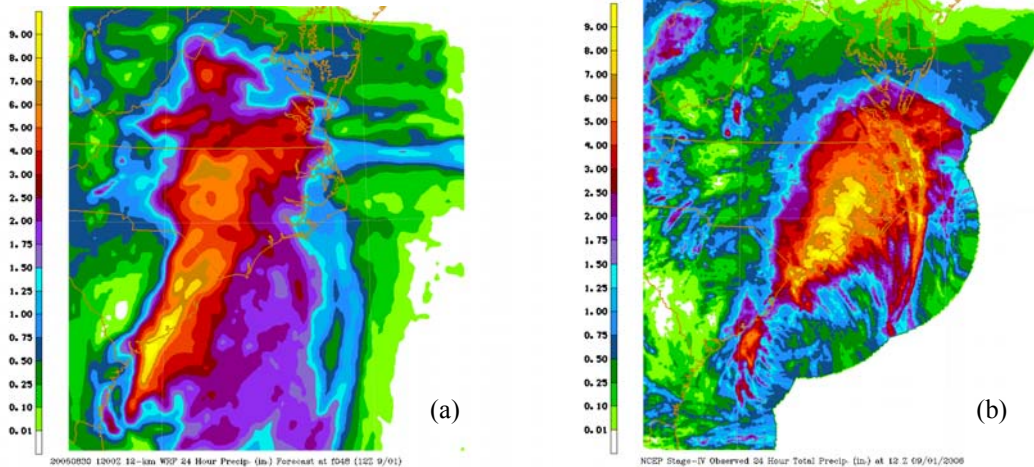


Figure 3.15. Comparison of (a) WRF control simulation QPF and (b) Stage IV QPE for 24-h period ending 12 UTC 1 September 2006.

Identifying the cause of the westward shift of Ernesto’s track was an important focus of subsequent work. One hypothesis was that this track bias depended on errors on the model initial condition. Another hypothesis was that model physics choices could have influenced the track. However, ensemble predictions with a variety of physics and initial conditions all exhibit this westward bias (Fig. 3.16).

As mentioned above, the PRE event appears to have reinforced the southward position of the frontal boundary, and also may have contributed to the formation of a weak CAD event. This would suggest that the cause of the westward track bias for Ernesto in model forecasts and simulations could be due to the lack of CAD, which would then be related to the limited representation of the PRE. Thus, our working hypothesis is that the lack of model ability to capture the PRE and subsequent CAD event led to the underestimate of a synoptic and mesoscale feature that helped to steer the observed track eastward, explaining the model westward track bias. Initial steps to test this hypothesis were to utilize the CAD-identification algorithm of Bailey et al. (2003) for both observations and model forecasts. This comparison revealed that CAD was present in the observations, while CAD was not fully present in model forecasts or simulations (Fig. 3.17).



Figure 3.16. Tracks of WRF simulations compared to NHC best track (white).

These findings led to the hypothesis that poor model representation of the PRE led to a lack of CAD in the model forecast. Poor model representation of CAD then led to an incorrect placement of the frontal boundary, perhaps resulting in the TC track and precipitation distribution error in the model forecast. Another question also arose as to what role the TC played in enhancing rainfall in the PRE through moisture transport (as suggested by prior research). Since TCs act as moisture sinks that remove water vapor from the surrounding environment, it is hypothesized that in some cases the TC *does not* enhance moisture or precipitation associated with PREs in downstream locations. Understanding the variable roles of TCs in PRE situations is an important operational objective.

In order to address the role of the TC in enhancing rainfall in the PRE through moisture transport, the TC vortex was removed using the TC Bogus Scheme in WRF (Fig. 3.18). While the TC vortex was successfully removed, much of the moisture remained in the surrounding environment with high precipitable water values greater than 2 in (50 mm) over the PRE region (Fig. 3.19). When comparing the 24-hour precipitation forecast ending at 12 UTC 31 August 2006 after the PRE event dissipated, both the location and magnitude of precipitation totals are very similar within the PRE region, *even without Ernesto* (Fig. 3.20). These results indicate that removal of the TC appears to cause little change to the PRE and that the TC plays a limited role in enhancing rainfall for this PRE event.

YEARMODAHRRMN	Line A	Line B	Line C	Line D					
200608310454	1	1	1	1	200608310400	0	0	1	0
200608310554	1	1	1	1	200608310500	0	0	1	0
200608310654	1	1	1	1	200608310600	0	0	1	0
200608310754	1	1	1	1	200608310700	1	0	1	0
200608310854	1	1	1	1	200608310800	0	0	1	0
200608310954	1	1	1	1	200608310900	1	0	1	0
200608311054	1	1	1	1	200608311000	0	0	0	1
200608311154	1	1	1	1	200608311100	0	0	0	1
200608311254	1	1	1	1	200608311200	0	0	0	1
200608311354	1	1	1	1	200608311300	1	1	0	1
					200608311400	1	0	0	1

Figure 3.17. Comparison of CAD algorithm results from surface observations (left) with WRF control simulation (right). Values of 1 correspond to meeting of CAD criteria, and the different columns correspond to the different section lines utilized in the Bailey et al. (2003) CAD-detection algorithm. Green shading indicates that each line met the CAD conditions, while yellow shading indicates that CAD conditions were only partially met.

As previously mentioned, Fig. 3.17 indicates that while CAD was observed, the model failed to adequately simulate CAD from 05 to 14 UTC 31 August 2006 following the PRE. A WRF simulation with no terrain was completed to determine what role terrain might have played in forcing CAD and modulating the precipitation distribution. When comparing the TC tracks from the 36, 12, and 4-km domains of the experimental no terrain run to the control run, the tracks are very similar until reaching the North Carolina-Virginia border where the no terrain run tracks have a greater westward deviation (Fig. 3.21). Likewise, the precipitation distribution for the no terrain run shows a westward shift in precipitation inland over West Virginia (Fig. 3.22). However, there is an eastward shift in precipitation over North Carolina for the no terrain run shortly after the time of landfall. These results indicate that terrain does play a role in modulating precipitation distribution. However, its relationship to CAD representation in the model forecast remains unclear.

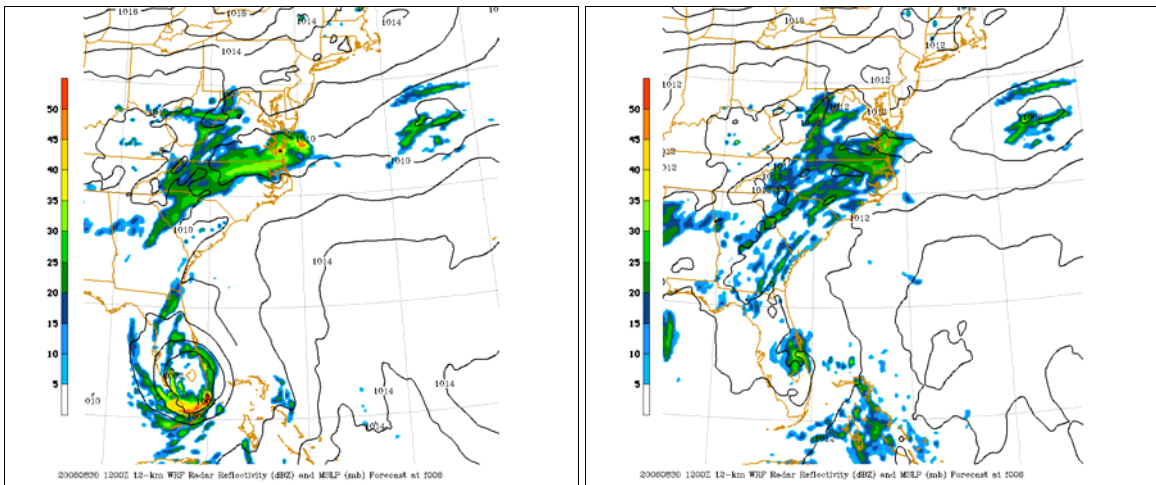


Figure 3.18. Comparison of radar reflectivity (dBZ) and MSLP (mb) forecast at 18 UTC 30 August 2006 from control simulation (left) and no TC simulation (right). Plots are for 12-km domain.

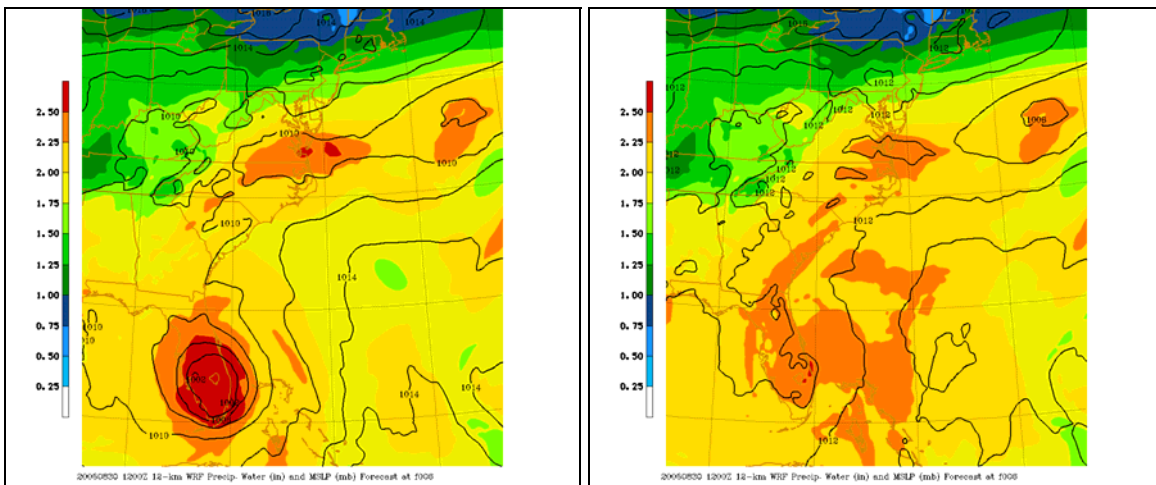


Figure 3.19. Comparison of precipitable water (in) and MSLP (mb) forecast at 18 UTC 30 August 2006 from control simulation (left) and no TC simulation (right). Plots are for 12-km domain.

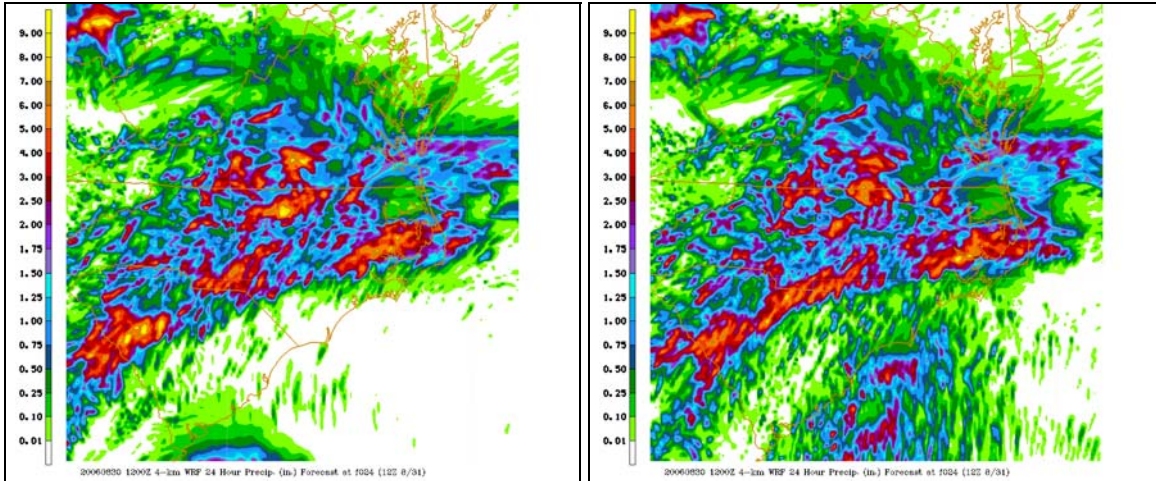


Figure 3.20. Comparison of 24-hour precipitation forecast (in) and MSLP (mb) forecast at 12 UTC 31 August 2006 from control simulation (left) and experimental no TC simulation (right). Plots are for 4-km grid spacing domains.



Figure 3.21. Tracks of WRF control run forecasts (blue: 36-km domain, green: 12-km domain, and purple: 4-km domain) compared to no terrain run forecasts (red: 36-km domain, orange: 12-km domain, and yellow: 4-km domain) and NHC best track (white).

Determining the role of CAD in modulating the precipitation distribution and track of TC Ernesto in model forecasts requires an experimental run with adequate model representation of CAD for comparison to the control run, which had poor CAD representation. When comparing model forecasts of relative humidity in the control run to observed relative humidity at the time of PRE initiation, the control run had higher relative humidity over the Piedmont region of North Carolina and Virginia and lower relative humidity over eastern North Carolina when compared to the observed relative humidity.

By lowering the relative humidity in the lower troposphere over the Piedmont region of North Carolina and Virginia, increased evaporational cooling associated with the PRE is expected to enhance the intensity of CAD in the model forecasts. The resulting precipitation distribution and track of TC Ernesto can then be compared to the control run to determine what role CAD might play in the westward bias of the model forecasts. These results (not shown here) proved inconclusive; see Dale (2013) for details.

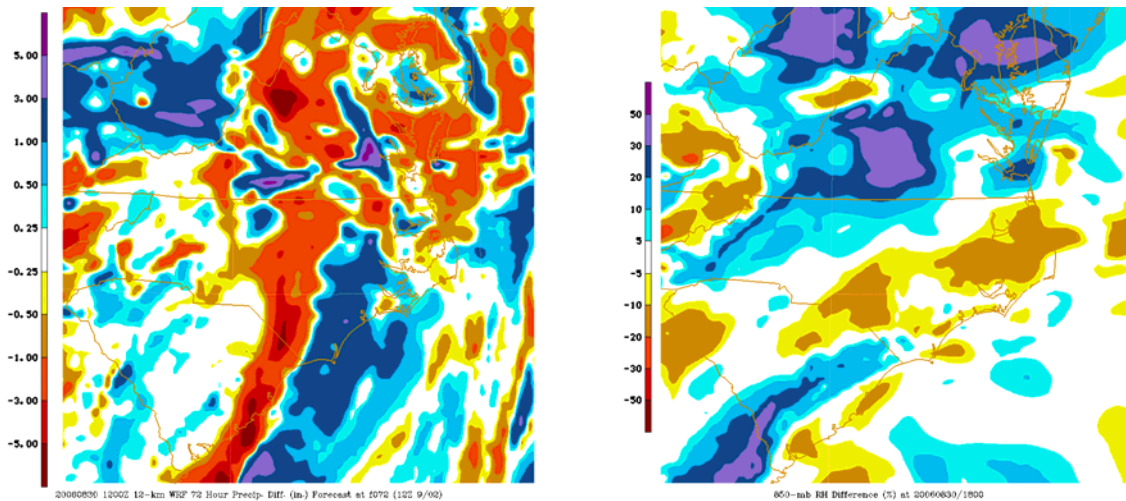


Figure 3.22. (a) 12-km domain 72-hr precipitation difference forecast (no terrain run - control run) ending at 12 UTC 02 September 2006; (b) 12-km domain 850-mb relative humidity difference forecast (WRF control run - RUC analysis) at the time of PRE initiation, 18 UTC 30 August 2006.

Collaborative research on Tropical Storm Hanna

NWS Raleigh forecaster Barrett Smith has been conducting simulations of Tropical Storm Hannah (2008) in order to better understand the role of a boundary feature in focusing the heavy precipitation across North Carolina in that event. Barrett and PI Lackmann discussed a series of model experiments that are designed to elucidate the importance of lower-tropospheric boundaries to both precipitation and surface wind speeds.

Because Hanna was relatively weak at the time of model initialization, it was relatively easy to obtain realistic control simulations using the WRF-ARW model. These model runs were able to adequately reproduce the swath of heavy precipitation across central North Carolina (not shown). It was hypothesized that a weak boundary, formed in part due to evaporational cooling towards the cool side of the front, acted to increase the precipitation via isentropic lift on the cool side of the boundary. Furthermore, the stable lower troposphere on the cool side of the boundary would inhibit vertical mixing and may serve to diminish peak wind speeds there. In order to test these hypotheses, experimental simulations in which evaporational cooling was omitted were conducted. These simulations reveal a weakening and shift of the precipitation swath, and also exhibit stronger surface winds in the vicinity of the stable layer (to the left of the track of the storm center, Fig. 3.23). However, the magnitude of the changes was less than expected. Interestingly, later in the model run, Hanna weakens more in the no-evaporation simulation, and wind speeds diminish due to that effect beyond hour 62 of the simulation (not shown).

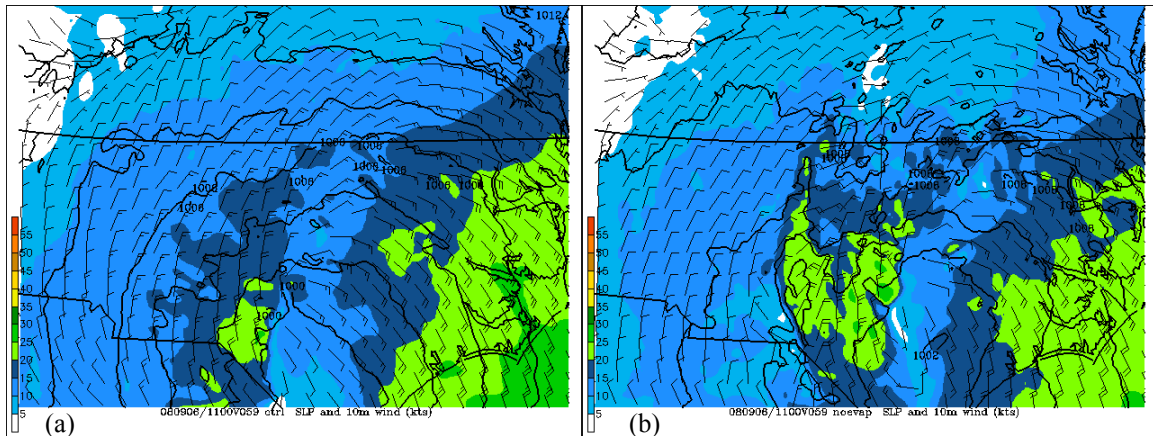


Figure 3.23. Comparison of sea level pressure (solid contours, 2 hPa interval) and 10-m wind speed (kt, shaded as in legend at left of panel) for hour 59 of the simulations (valid 11 UTC 6 Sept 2008); (a) control simulation, (b) experimental simulation without evaporational cooling.

Summary of accomplishments:

- A method of improved initial conditions has been developed by graduate student Briana Gordon and Dr. Etherton. Initial efforts using the GFDL bogus vortex approach did not yield satisfactory results, necessitating use of data assimilation (DA) approaches. A hybrid ensemble Kalman filter (EnKF) approach was devised and tested for the case of Hurricane Earl (2010).
- Gary Lackmann presented a webinar on 5 July 2012 outlining the TC initialization process in current NCEP models, including the GFS upgrade of 22 May 2012. Assistance from Daryl Kleist (EMC), Mike Brennan (NHC), and John Brown (ESRL) provided up-to-date information and examples.
- Removal of the TC in WRF model forecasts indicates *the TC played a minimal role in enhancing rainfall associated with the PRE in this case.*
- Lack of CAD in model forecasts does not appear to be related to terrain. However, terrain does play a role in modulating the TC track and precipitation distribution for this case.
- The frequency of CAD during landfalling TC events in the Southeastern United States was further investigated by NWS collaborator Barrett Smith. Using the CAD-detection algorithm from Bailey et al. (2003), Smith found cases of CAD preceding TC landfall to occur with 50% of landfalling TC cases from 1995 to 2012 in the Southeastern United States.
- A presentation summarizing the research was presented at the 37th NWA conference in Madison WI in October 2012 and the NWS Eastern Region Virtual Conference on March 12, 2013.

C. Other project information

1.) Collaborative Investigators

The following is a listing of the NWS CI personnel associated with each research area.

Tropical cyclone winds

PI - Dr Anantha Aiyyer

Student - Bryce Tyner

Lead CI - Reid Hawkins Donald.Hawkins@noaa.gov (ILM)

Lead CI Assistant - David Glenn David.Glenn@noaa.gov (MHX)

Other CIs -

John Billet John.Billet@noaa.gov (AKQ)

Chris Wamsley Chris.Wamsley@noaa.gov (AKQ)

Robert Bright Robert.Bright@noaa.gov (CHS)

Frank Alsheimer Frank.Alsheimer@noaa.gov (CHS)

Thomas J LeFebvre Thomas.J.Lefebvre@noaa.gov (GSD)

David Roth David.Roth@noaa.gov (HPC)

David Glenn david.glenn@noaa.gov (MHX)

Gail Hartfield Gail.Hartfield@noaa.gov (RAH)

Jonathan Blaes Jonathan.Blaes@noaa.gov (RAH)

Michael Brennan Michael.J.Brennan@noaa.gov (TPC)

Tropical Cyclone Model Initialization and Precipitation

PI - Dr Gary Lackmann and Dr Brian Etherton (BE for year 1 only)

Students – Briana Gordon and Jordan Dale

Lead CI – Barrett Smith Barrett.Smith@noaa.gov (RAH)

Lead CI Assistant – Jim Hudgins James.Hudgins@noaa.gov (RNK)

Other CIs -

John Billet John.Billet@noaa.gov (AKQ)

Eric Seymour eric.seymour@noaa.gov (AKQ)

Frank Alsheimer Frank.Alsheimer@noaa.gov (CHS)

Daryl Kleist daryl.kleist@noaa.gov (EMC)

David Roth David.Roth@noaa.gov (HPC)

Sim Aberson Sim.Aberson@noaa.gov (HRD)

Jonathan Blaes Jonathan.Blaes@noaa.gov (RAH)

Jack Bushong Jack.Bushong@noaa.gov (SERFC)

High Shear/Low CAPE

PI - Dr Mathew Parker

Students – Jason Davis and Keith Sherburn

Lead CI Pat Moore Pat.Moore@noaa.gov (GSP)

Lead CI Assistant Justin Lane Justin.Lane@noaa.gov (GSP)

Lead CI Assistant Hunter Coleman Hunter.Coleman@noaa.gov (CAE)

Other CIs -

Andrew Zimmerman Andrew.Zimmerman@noaa.gov (AKQ)

Michael Cammarata Michael.Cammarata@noaa.gov (CAE)

Shawn Smith Shawn.Smith@noaa.gov (CAE)

Wendy Sellers wendy.sellers@noaa.gov (CHS)

Steven Nelson Steven.Nelson@noaa.gov (FFC)

Trisha Palmer trisha.palmer@noaa.gov (FFC)
Harry Gerapetritis Harry.Gerapetritis@noaa.gov (GSP)
Andy Kula Andy.Kula@noaa.gov (HUN)
Kurt Weber Kurt.Weber@noaa.gov (HUN)
Stephen Latimer Stephen.Latimer@noaa.gov (HUN)
Steven Zubrick Steven.Zubrick@noaa.gov (LWX)
Robert Frederick Robert.Frederick@noaa.gov (MHX)
Steve Keighton Stephen.Keighton@noaa.gov (RNK)
Jonathan Blaes Jonathan.Blaes@noaa.gov (RAH)
Michael Strickler michael.strickler@noaa.gov (RAH)
Steven Weiss steven.j.weiss@noaa.gov (SPC)
Russell Schneider Russell.Schneider@noaa.gov (SPC)
Andy Dean Andy.Dean@noaa.gov (SPC)

High-Resolution Mesoscale Ensemble

PI- Dr Brian Etherton Brian.Etherton@noaa.gov (NCSU | GSD)
CI- Michael Cammarata Michael.Cammarata@noaa.gov (CAE)
Frank Alsheimer Frank.Alsheimer@noaa.gov (CHS)
Reid Hawkins Donald.Hawkins@noaa.gov (ILM)
Steven Zubrick Steven.Zubrick@noaa.gov (LWX)
Barrett Smith Barrett.Smith@noaa.gov (RAH)
Jonathan Blaes Jonathan.Blaes@noaa.gov (RAH)
Steve Keighton Stephen.Keighton@noaa.gov (RNK)

2.) Conference presentations, workshops, NWS webinars, and Seminars

Conferences:

2014 AMS Annual Meeting, Atlanta, GA

Jordan Dale presented "The Role of Hurricane Ernesto (2006) in a Predecessor Rainfall Event" at the 26th Conference on Weather Analysis and Forecasting / 22nd Conference on Numerical Weather Prediction, Atlanta, GA, February 2014.

2013 AMS Student Conference

Keith Sherburn presented "The High Shear/Low CAPE Problem: Improving Detection of Significant Weather Events in Marginally Unstable Environments" at the 12th Annual Student Conference at the 93rd AMS Annual Meeting, Austin, TX, January 2013.

26th Conference on Severe Local Storms

Jason Davis presented "Radar Climatology of Tornadoes Occurring in High Shear/Low CAPE Environments in the Mid-Atlantic and Southeast" at the 26th Conference on Severe Local Storms, Nashville, TN, November 2012.

26th Conference on Severe Local Storms

Keith Sherburn presented "Identifying Discriminating Environmental Features Between High Shear/Low CAPE Severe Convection and Null Events" at the 26th Conference on Severe Local Storms, Nashville, TN, November 2012.

2012 NWA Annual Meeting

Barrett Smith presented "Hurricane Ernesto (2006): Frontal Influence on Precipitation Distribution" at the 37th NWA Annual Meeting, Madison, WI, October 2012

2012 Conference on Hurricanes and Tropical Meteorology

Bryce Tyner presented "A Statistical and Numerical Modeling Approach to Improved Landfalling Tropical Cyclone Wind Forecasts" at the 30th Conference on Hurricanes and Tropical Meteorology, April 2012.

2012 AMS Annual Meeting, New Orleans, LA

Bryce Tyner presented "A New Approach to Improved Inland Wind Forecasts for Landfalling Tropical Cyclones" at the 92nd AMS Annual Meeting, January 2012.

CSTAR Workshops:

2012 CSTAR Virtual Workshop

In November 2012, a total of 45 meteorologists from the National Weather Service (NWS) as well as faculty and students from NC State University (NC SU) gathered via a virtual workshop to continue implementation of an ongoing Collaborative Science, Technology, and Applied Research (CSTAR) project. Despite travel limitations, 17 different offices or organizations participated virtually or in person with 13 attendees participating on site in Raleigh. Participants were from 11 different WFOs, 1 RFC, 3 national centers, 1 regional headquarters, and NC State University with 14 offices or organizations having at least 2 participants.

NWS Webinars:

NWS Eastern Region Fall Science Sharing Webinar October 2013

Jonathan Blaes presented "Developing a Data-set of Wind Gust Factors to Improve Forecasts of Wind Gusts in Tropical Cyclones" at the 2013 NWS Eastern Region Fall Science Sharing Webinar.

NWS Eastern Region Fall Science Sharing Webinar October 2012

Jordan Dale presented "Hurricane Ernesto (2006): Frontal Influence on Precipitation Distribution" at the 2012 NWS Eastern Region Fall Science Sharing Webinar.

NWS Eastern Region Hurricane Season Preparation Webinar April 2012

Bryce Tyner and Reid Hawkins presented an update on the Tropical Cyclone Inland Winds CSTAR project at the WFO CHS Tropical Weather Workshop. The presentation showed some of the problems facing forecasters and the limitations of the TCM guidance, and then shared some of the initial results including NDFD TC wind verification which notes a consistent high bias in WFO wind forecasts during TC's and some initial guidance on land reduction and gust factors

Improving the Forecasting of Severe Weather in High Shear, Low CAPE Environments Webinar October 2013

In October 2013, Keith Sherburn and Jason Davis shared their research results from their CSTAR supported High Shear Low CAPE project via a WDTB sponsored webinar. The webinar entitled Improving Forecasting of High Shear, Low CAPE Severe Weather Environments was attended by a total of 62 different NWS facilities including 57 WFOs. The total audience exceeded 190 NWS meteorologists from all four NWS CONUS regions. The learning objectives for the webinar included:

- Identify issues associated with forecasting HSLC significant severe environments
- Assess current techniques and determine most skillful environmental parameters
- Identify benefits of the Severe Hazards in Environments with Reduced Buoyancy (SHERB) parameter over “traditional” composite parameters for “low LCL” HSLC environments
- Identify utility of applying the SHERB parameter to other HSLC regimes

Improving the Forecasting of Severe Weather in High Shear, Low CAPE Environments Webinar April 2014

Jason Davis and Keith Sherburn delivered an additional webinar presentation entitled "Improving the Forecasting of Severe Weather in High Shear, Low CAPE Environments" on April 15, 2014. This presentation was attended by 29 different NWS offices.

Seminars:

July 2012 Marine Earth and Atmospheric Sciences Graduate Seminar

Jason Davis presented "Radar Climatology of Tornadic and Non-tornadic Vortices in High Shear, Low CAPE Environments in the Mid-Atlantic and Southeast" at a graduate student seminar.

May 2012 Marine Earth and Atmospheric Sciences Graduate Seminar

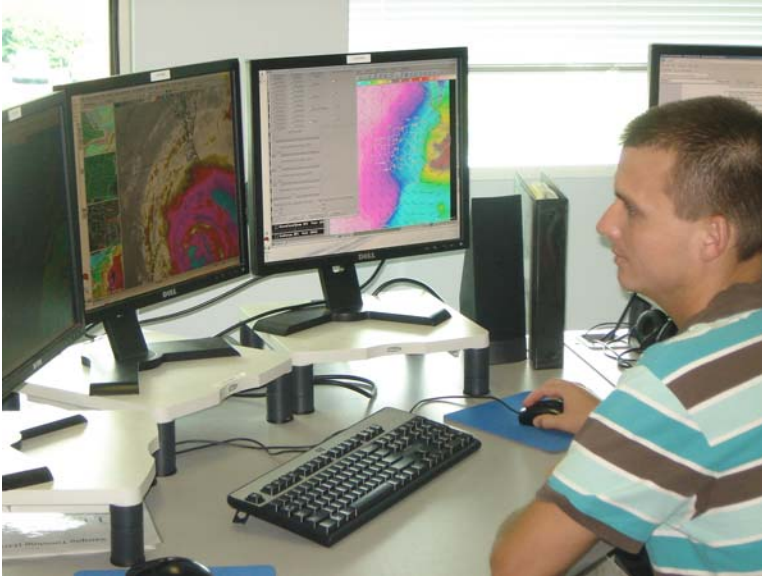
Keith Sherburn presented "Climatology and Ingredients of Significant Severe Convection in High Shear, Low CAPE Environments" at a graduate student seminar.

3.) Other project activity

The list of interesting or noteworthy activities below is provided to highlight topics that may not be captured in the detailed summaries provided by the PIs and students. Information on the research results, process, and findings are expected to be provided elsewhere.

Collocation with WFO was a Great Asset During Hurricane Irene

A real-time case study approach was taken during the landfall of Hurricane Irene in late August, 2011. Both the inland wind aspect and the precipitation forecast were monitored, and graduate student Bryce Tyner was present in the Raleigh forecast office to observe preparation of the wind forecasts (see photo below). The ability to observe and interact with operational forecasters was a tremendous asset to Bryce.



HSLC Students Visit WFO GSP in January 2011

NCSU students Jason Davis and Keith Sherburn visited WFO Greer, SC (GSP) to discuss a variety of topics related to the HSLC portion of the CSTAR project. The students met primarily with Pat Moore, Justin Lane, and Larry Lee from GSP and Hunter Coleman from WFO Columbia, SC (CAE). <http://cimmse.wordpress.com/2012/02/07/ncsu-students-visit-gsp/>

Two NC State CSTAR Students Presented with AMS Graduate Fellowships

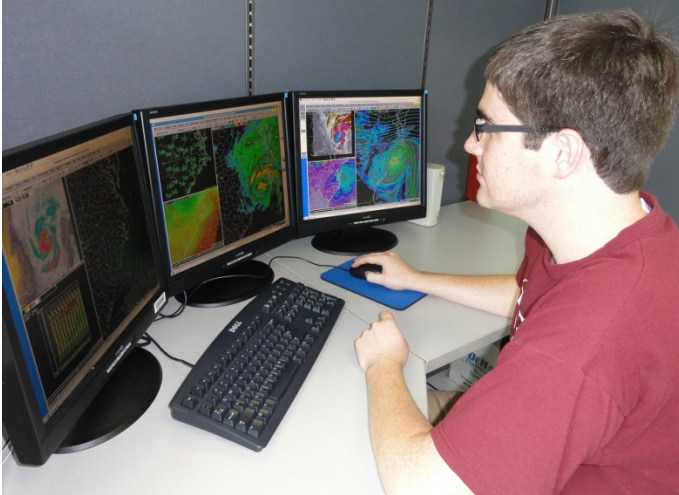
Jason Davis and Keith Sherburn were both formally presented with their 2011 American Meteorological Society (AMS) Graduate Fellowships this week at the 92nd Annual AMS Meeting in New Orleans. Jason Davis was awarded with the fellowship sponsored by the NASA Earth Science Program and Keith Sherburn was presented with the fellowship sponsored by NOAA's National Weather Service. In the photo below, Keith was congratulated by NWS Director Dr. Jack Hayes as this year's recipient of the AMS Student Fellowship sponsored by NOAA's National Weather Service.



Jordan Dale Utilizes the Weather Event Simulator at WFO RAH

Jordan Dale visited WFO Raleigh on several occasions in April and May to utilize the Weather Event Simulator (WES) to view data from Tropical Storm Ernesto. During these visits, Jordan utilized archived observational data provided by several WFOs. His analysis of the surface fields including manual surface analysis based on maps generated from the WES were recently shared on the CIMMSE blog where he provided an update.

<http://cimmse.wordpress.com/2012/05/09/tc-boundaryqpf-hurricane-ernesto-case-study-update/>



TC Wind Project Collaborating with the Tropical Hazards Team and GFE Developers

At the 2011 NOAA Hurricane Conference, WFO RAH requested that the Tropical Hazards Team and GFE developers work with the CSTAR group to add additional science and improve collaboration in the creation of wind and wind gust grids associated with tropical cyclones by updating the TCMWindTool and creating a new TCWindGustTool. The CSTAR group has begun collaborating with the Tropical Hazards Team to add more rigorous science and results from this project to the TCMWindTool documentation and reference materials with the eventual goal of developing new tools for use in GFE.

Three CSTAR Students Complete Student Internship at WFO RAH

Jason Davis, Keith Sherburn, and Jordan Dale recently completed their summer long student internship at WFO Raleigh. During the semester the students "shadowed" NWS staff, performing routine NWS duties, assisting NWS staff during active weather events, participating in NWS training activities, conducting site visits to the KRAX Doppler radar and an ASOS station, participating in a Weather Event Simulation, and learning about the federal job application process.

Keith Sherburn summarized the importance of the internship with his research: "During the course, I was able to see day-to-day NWS operations through the eyes of forecasters, providing insights on available resources, office practices, and general situational awareness. Since taking the course, my research mindset has gained a more substantial operational component, leading me to ask myself through every step of the process, "How will this help the NWS better serve the public?" As a result, I believe my research, once completed, will provide an even greater benefit to operational forecasters than it would have without this additional experience at WFO Raleigh."

NC State CSTAR Projects Deliver Large Numbers of Skilled NOAA Employees

An examination of the students who have participated in the three NC State CSTAR projects that have been completed shows that 17 former CSTAR students are currently employed in NOAA or as a NOAA contractor. A total of ten of these former students are currently employed at WFOs from Alaska to South Carolina, one at an RFC, three at NCEP, and one at OAR/ESRL. In addition, two former principal investigators are currently employed at NOAA OAR facilities.

<http://cimmse.wordpress.com/2012/04/11/nc-state-cstar-projects-deliver-large-numbers-of-skilled-noaa-employees/>

Contributions to the National CSTAR Program

The NC State-NWS CSTAR group supported the NWS CSTAR program by providing materials for presentations by Curtis Marshal titled “The CSTAR Program” which were shared at the March Research and Innovation Transition Team Forum and at the 2nd NOAA Testbed Workshop at the Earth System Research Laboratory.

Hurricane Sandy Provides the First Opportunity to Test and Develop New Tropical Cyclone Wind and Wind Gust Tools

Based on research associated with the inland wind portion of this project, collaborators are developing new smart tools and grids to use in the Gridded Forecast Editor (GFE). Hurricane Sandy provided the first opportunity to test and evaluate some of these new GFE tools and methodologies with a real storm. The testing took place at WFOs ILM, MHX, and RAH. Lead Forecaster Scott Sharp at WFO RAH used the new TCWindGust smart tool to create Wind Gust grids during the time in which Sandy influenced the NC coast. Scott used the “CSTAR Regression” option with the tool and was happy with the result. The tool and the research project was noted in the Area Forecast Discussion (see below). In addition, the real-time evaluation resulted in additional tool development as WFO ILM created a new tool to that allows forecasters to assign wind reduction factors more efficiently.

AS SANDY MOVES **NWD** OFFSHORE OF SC-**NC** LATE SATURDAY THROUGH EARLY SUNDAY...**EXPECT TO SEE AN INCREASE IN THE WINDS...ESPECIALLY AFTER MIDNIGHT SATURDAY NIGHT WHEN SANDY MAKES ITS CLOSEST APPROACH TO THE NC COAST (THOUGH STILL QUITE A DISTANCE OFFSHORE). POPULATED THE WIND GRIDS WITH TCM WINDS FROM THE LATEST NHC TCM PRODUCT THEN USED A REDUCTION FACTOR OF 30 PERCENT DUE TO SURFACE FRICTION. GUSTS ACHIEVED BY UTILIZING RESEARCH CURRENTLY BEING CONDUCTED BY THE C*STAR INITIATIVE (COLLABORATION BETWEEN NWS AND LOCAL UNIVERSITIES). CURRENTLY EXPECT MAX GUSTS IN OUR FAR EASTERN COASTAL PLAIN COUNTIES EARLY SUNDAY MORNING 30-33KTS.**

CSTAR Tropical Cyclone Wind Project Noted and Supported in the NWS Hurricane Irene Service Assessment

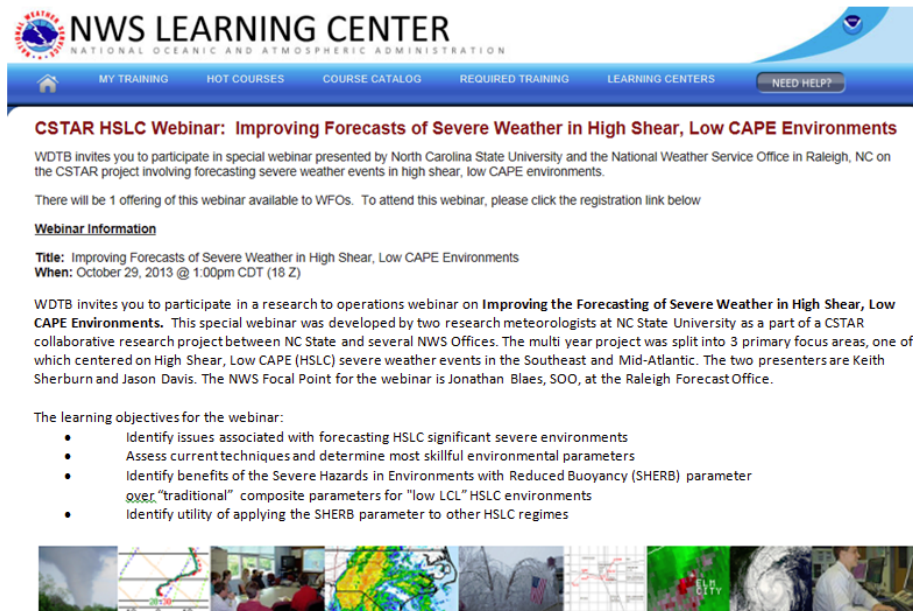
The NC State-NWS Raleigh CSTAR project was noted in recommendation 54 of the NWS Hurricane Irene Service Assessment. The full text of the recommendation is shown below along with a link to the entire service assessment.

Recommendation 54 (Strategic): In addition to the need for better estimates of surface wind speeds/intensity in tropical cyclones prior to landfall (see Recommendation 43), WFOs in close collaboration with NHC and their neighboring and backup offices, should apply meteorologically appropriate inland surface wind speed reductions as opposed to a blanket wind reduction. NWS should support research such as the NOAA Collaborative Science, Technology, and Applied Research (CSTAR) project, “Improving Understanding and Prediction of Hazardous Weather in the Southeastern United States: Landfalling Tropical Cyclones and Convective Storms.” This change will likely require the development of a more robust and scientifically sound smart tool that applies spatially varying wind reductions that more appropriately account for boundary layer meteorology and topography.

The NWS Hurricane Irene Service Assessment is available at the following URL: <http://www.nws.noaa.gov/om/assessments/pdfs/Irene2012.pdf>

CSTAR High Shear Low CAPE Project Collaborates with the WDTB

The CSTAR High Shear Low CAPE (HSLC) project collaborated with the Warning Decision training Branch (WDTB) to share research results from the HSLC project. This was the first time that an NC State CSTAR project utilized the resources and assistance of the WDTB. The resulting webinar was attended by a total of 62 different NWS facilities including 57 WFOs. The total audience exceeded 190 NWS meteorologists from all four NWS CONUS regions.



NWS LEARNING CENTER
NATIONAL OCEANIC AND ATMOSPHERIC ADMINISTRATION

MY TRAINING HOT COURSES COURSE CATALOG REQUIRED TRAINING LEARNING CENTERS NEED HELP

CSTAR HSLC Webinar: Improving Forecasts of Severe Weather in High Shear, Low CAPE Environments

WDTB invites you to participate in special webinar presented by North Carolina State University and the National Weather Service Office in Raleigh, NC on the CSTAR project involving forecasting severe weather events in high shear, low CAPE environments.

There will be 1 offering of this webinar available to WFOs. To attend this webinar, please click the registration link below

Webinar Information

Title: Improving Forecasts of Severe Weather in High Shear, Low CAPE Environments
When: October 29, 2013 @ 1:00pm CDT (18 Z)

WDTB invites you to participate in a research to operations webinar on **Improving the Forecasting of Severe Weather in High Shear, Low CAPE Environments**. This special webinar was developed by two research meteorologists at NC State University as a part of a CSTAR collaborative research project between NC State and several NWS Offices. The multi year project was split into 3 primary focus areas, one of which centered on High Shear, Low CAPE (HSLC) severe weather events in the Southeast and Mid-Atlantic. The two presenters are Keith Sherburn and Jason Davis. The NWS Focal Point for the webinar is Jonathan Blaes, SOO, at the Raleigh Forecast Office.

The learning objectives for the webinar:

- Identify issues associated with forecasting HSLC significant severe environments
- Assess current techniques and determine most skillful environmental parameters
- Identify benefits of the Severe Hazards in Environments with Reduced Buoyancy (SHERB) parameter over "traditional" composite parameters for "low LCL" HSLC environments
- Identify utility of applying the SHERB parameter to other HSLC regimes



CSTAR Research to Operations Gains Support at 2013 NOAA Hurricane Conference

The NC State-NWS CSTAR tropical cyclone winds team provided an update on their research and collaborative activities at the 2013 NOAA Hurricane Conference. The CSTAR agenda item was received favorably and additional resources were provided to the project. Participants from NWS Weather Forecast Offices (WFOs), the National Hurricane Center (NHC), the Hurricane Research Division, the Earth Systems Research Laboratory (ESRL) collaborated and implemented the CSTAR research during the 2014 Hurricane Season.

D. References

- Atkins, N. T., and M. St. Laurent, 2009: Bow echo mesovortices. Part I: Processes that influence their damaging potential. *Mon. Wea. Rev.*, **137**, 1497–1513.
- Atkins, N. T., J. M. Arnott, R. W. Przybylinski, R. A. Wolf, and B. D. Ketcham, 2004: Vortex structure and evolution within bow echoes. Part I: Single-Doppler and damage analysis of the 29 June 1998 derecho. *Mon. Wea. Rev.*, **132**, 2224–2242.
- Atkins, N. T., C. S. Bouchard, R. W. Przybylinski, R. J. Trapp, and G. Schmocker, 2005: Damaging surface wind mechanisms within the 10 June 2003 Saint Louis bow echo during BAMEX. *Mon. Wea. Rev.*, **133**, 2275–2296.
- Bailey, C. M., G. Hartfield, G. M. Lackmann, K. Keeter, and S. Sharp, 2003: An objective climatology, classification scheme, and assessment of sensible weather impacts for Appalachian cold-air damming. *Wea. Forecasting*, **18**, 641–661.
- Burke, P. C., and D. M. Schultz, 2004: A 4-Yr climatology of cold-season bow echoes over the continental United States. *Wea. Forecasting*, **19**, 1061–1074.
- Dale, F. J., 2013: Diagnosing processes modulating precipitation distribution during landfalling tropical cyclones in the Carolinas and Virginia. Thesis, Dept. of Marine, Earth, and Atmospheric Sciences, North Carolina State University, 167 pp. [Available online at: <http://repository.lib.ncsu.edu/ir/handle/1840.16/9025>]
- Davies, J. M., 1990: Midget supercell spawns tornadoes. *Weatherwise*, **43** (10), 260–261.
- Davis, C., W. Wang, S. S. Chen, Y. Chen, K. Corbosiero, M. DeMaria, J. Dudhia, G. Holland, J. Klemp, J. Michalakes, H. Reeves, R. Rotunno, C. Snyder, and Q. Xiao, 2008: Prediction of landfalling hurricanes with the Advanced Hurricane WRF Model. *Mon. Wea. Rev.* **136**, 1990–2005.
- Davis, J. M. 2013: Radar climatology of tornadic and non-tornadic vortices in high shear, low CAPE environments in the Mid-Atlantic and Southeast. Thesis, Dept. of Marine, Earth, and Atmospheric Sciences, North Carolina State University, 151 pp. [Available online at: <http://repository.lib.ncsu.edu/ir/handle/1840.16/8921>]
- Davis, J. M., and M. D. Parker, 2014: Radar climatology of tornadic and non-tornadic vortices in high shear, low CAPE environments in the mid-Atlantic and southeastern U.S. *Wea. Forecasting*, accepted in final form, April 2014. *In press*. <http://journals.ametsoc.org/doi/abs/10.1175/WAF-D-13-00127.1>
- Funk, T.W., K.E. Darmofal, J.D. Kirkpatrick, V.L. DeWald, R.W. Przybylinski, G.K. Schmocker, and Y.J. Lin, 1999: Storm reflectivity and mesocyclone evolution associated with the 15 April 1994 squall line over Kentucky and Southern Indiana. *Wea. Forecasting*, **14**, 976–993.
- Galarneau, T. J., L. F. Bosart, and R. S. Schumacher, 2010: Predecessor rain events ahead of tropical cyclones. *Mon. Wea. Rev.*, **138**, 3272–3297.
- Gordon, B. J., 2011: The sensitivity of tropical cyclone forecast simulations in the WRF model to initial conditions. Thesis, Dept. of Marine, Earth, and Atmospheric Sciences, North Carolina State University, 137 pp. [Available online at:

<http://repository.lib.ncsu.edu/ir/bitstream/1840.16/7050/1/etd.pdf>

- Hart, R. E., 2008: Improved TC forecasting through initialization of MM5 with GFDL/GFS Merger. Preprint for the 28th Conference on Hurricanes and Tropical Meteorology. American Meteorological Society.
- Hill, K. A., and G. M. Lackmann, 2009a: Influence of environmental humidity on tropical cyclone size. *Mon. Wea. Rev.*, **137**, 3294–3315.
- Hsu, S. A., 2001: Statistical variations in gust factor across the coastal zone during Hurricane Opal in 1995. *Natl. Wea. Dig.*, **25**, 21–23.
- Kaplan, J. , and M. DeMaria, 1995: A simple empirical model for predicting the decay of tropical cyclone winds after landfall. *J. Appl. Meteor.*, **34**, 2499-2512.
- Kaplan, J., and M. DeMaria, 2001: On the decay of tropical cyclone winds after landfall in the New England Area. *J. Appl. Meteor.*, **40**, 280–286.
- Kennedy, P. C., N. E. Westcott, and R. W. Scott, 1993: Single-Doppler radar observations of a minisupercell tornadic thunderstorm. *Mon. Wea. Rev.*, **121**, 1860–1870.
- Kurihara, Y., M.A. Bender, and R.J. Ross, 1993: An initialization scheme of hurricane models by vortex specification. *Mon. Wea. Rev.*, **121**, 2030–2045.
- Lin, N., J. A. Smith, G. Villarini, T. P. Marchok, and M. L. Baeck, 2010: Modeling extreme rainfall, winds, and surge from Hurricane Isabel (2003). *Wea. Forecasting*, **25**, 1342–1361.
- McCaul, E.W., and M. L. Weisman, 1996: Simulation of shallow supercell storms in landfalling hurricane environments. *Mon. Wea. Rev.*, **124**, 408–429.
- Paulsen, B. and J. Schroeder, 2005: An Examination of Tropical and Extratropical Gust Factors and the Associated Wind Speed Histograms. *Journal of Applied Meteorology*, **44**, 270–280.
- Przybylinski, R.W., 1995: The Bow Echo: Observations, Numerical Simulations, and Severe Weather Detection Methods. *Wea. Forecasting*, **10**, 203–218.
- Schneider, R.S., A.R. Dean, S.J. Weiss, and P.D. Bothwell, 2006: Analysis of estimated environments for 2004 and 2005 severe convective storm reports. Preprints, 23rd Conf. Severe Local Storms, St. Louis MO, Amer. Meteor. Soc., 3.5.
- Schneider, R.S., and A.R. Dean, 2008: A comprehensive 5-year severe storm environment climatology for the continental United States. Preprints, 24th Conf. Severe Local Storms, Savannah GA, Amer. Meteor. Soc., 16A.4.
- Smith, B. T., R. L. Thompson, J. S. Grams, C. Broyles, and H. E. Brooks, 2012: Convective modes for significant severe thunderstorms in the contiguous United States. Part I: Storm classification and climatology. *Wea. Forecasting*, **27**, 1114–1135.
- Srock A. F., and L. F. Bosart, 2009: Heavy precipitation associated with southern Appalachian cold-air damming and Carolina coastal frontogenesis in advance of weak landfalling Tropical Storm Marco (1990). *Mon. Wea. Rev.* **137**, 2448–2470.
- Sherburn, K.D., 2013: Improving the understanding and forecasting of severe high shear, low CAPE environments. Thesis, Dept. of Marine, Earth, and Atmospheric Sciences, North Carolina State University, 124 pp. [Available online at: <http://www.lib.ncsu.edu/resolver/1840.16/8666>]

- Sherburn, K. D., and M. D. Parker, 2014: Climatology and ingredients of significant severe convection in high shear, low CAPE environments. *Wea. Forecasting*, accepted in final form, April 2014. *In press*. <http://journals.ametsoc.org/doi/abs/10.1175/WAF-D-13-00041.1>
- Tyner, Bryce, P. A. Aiyyer, J. Blaes, and D. R. Hawkins, 2014: An Examination of Wind Decay, Sustained Wind Speed Forecasts, and Gust Factors for Recent Tropical Cyclones in the Mid-Atlantic Region of the United States. *Wea. Forecasting*, revision submitted April 2014.
- Thompson, R. L., R. Edwards, and C. M. Mead, 2004: An update to the supercell composite and significant tornado parameters. Preprints, 22nd Conf. on Severe Local Storms, Hyannis, MA, Amer. Meteor. Soc., P8.1.
- Trapp, R.J., and M.L. Weisman, 2003: Low-Level Mesovortices within Squall Lines and Bow Echoes. Part II: Their Genesis and Implications. *Mon. Wea. Rev.*, **131**, 2804–2823.
- Trapp, R.J., S.A. Tessendorf, E.S. Godfrey, and H.E. Brooks, 2005: Tornadoes from squall lines and bow echoes. Part I: Climatological distribution. *Wea. Forecasting*, **20**, 23–34.
- Vickery, P. and P. Skerlj, 2005: Hurricane gust factors revisited. *J. Struct. Eng.*, **131**, 825–832.
- Wakimoto, R. M., 2001: Convectively driven high winds. *Severe Convective Storms, Meteor. Monogr.*, No. 50, Amer. Meteor. Soc., 255–298.
- Wakimoto, R.M., H.V. Murphey, C.A. Davis, and N.T. Atkins, 2006: High winds generated by bow echoes. Part II: The relationship between the mesovortices and damaging straight-line winds. *Mon. Wea. Rev.*, **134**, 2813–2829.
- Weisman, M.L., 1993: The genesis of severe, long-lived bow echoes. *J. Atmos. Sci.*, **50**, 645–670.
- Wheatley, D.M., R.J. Trapp, and N.T. Atkins, 2006: Radar and damage analysis of severe bow echoes observed during BAMEX. *Mon. Wea. Rev.*, **134**, 791–806.